NF1: A Model Tumor Suppressor Gene and So Much More!

Angela C Hirbe, M.D., Ph.D.

Division of Medical Oncology

Washington University School of Medicine

Siteman Cancer Center

Medical Oncology, Sarcoma Program

Neurofibromatosis Center

No Disclosures

Neurofibromatosis type 1 (NF1)

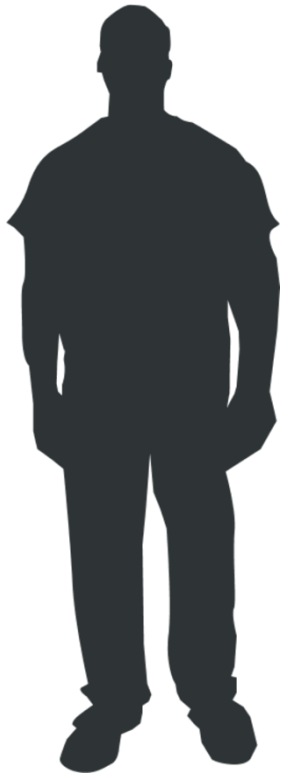

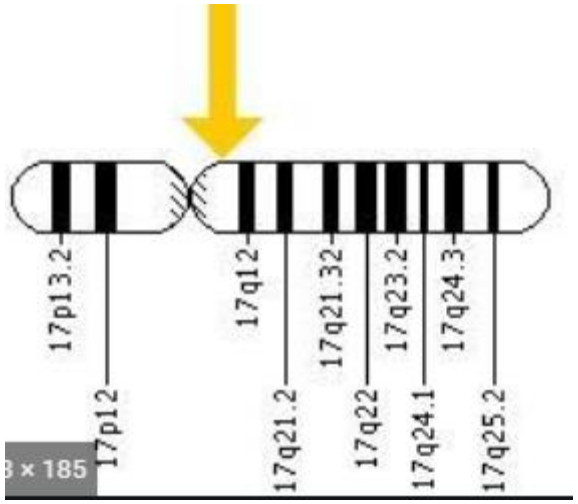

- Cancer predisposition syndrome caused by a germline mutation in the *NF1* gene
- Affects 1:2500 individuals worldwide
- Involves numerous organ systems
- The *NF1* gene is located on chromosome 17q11.2 and encodes for the protein neurofibromin
- This large gene (60 exons and >300 kilobases (kb) of genomic DNA) has one of the highest rates of spontaneous mutations in the entire human genome

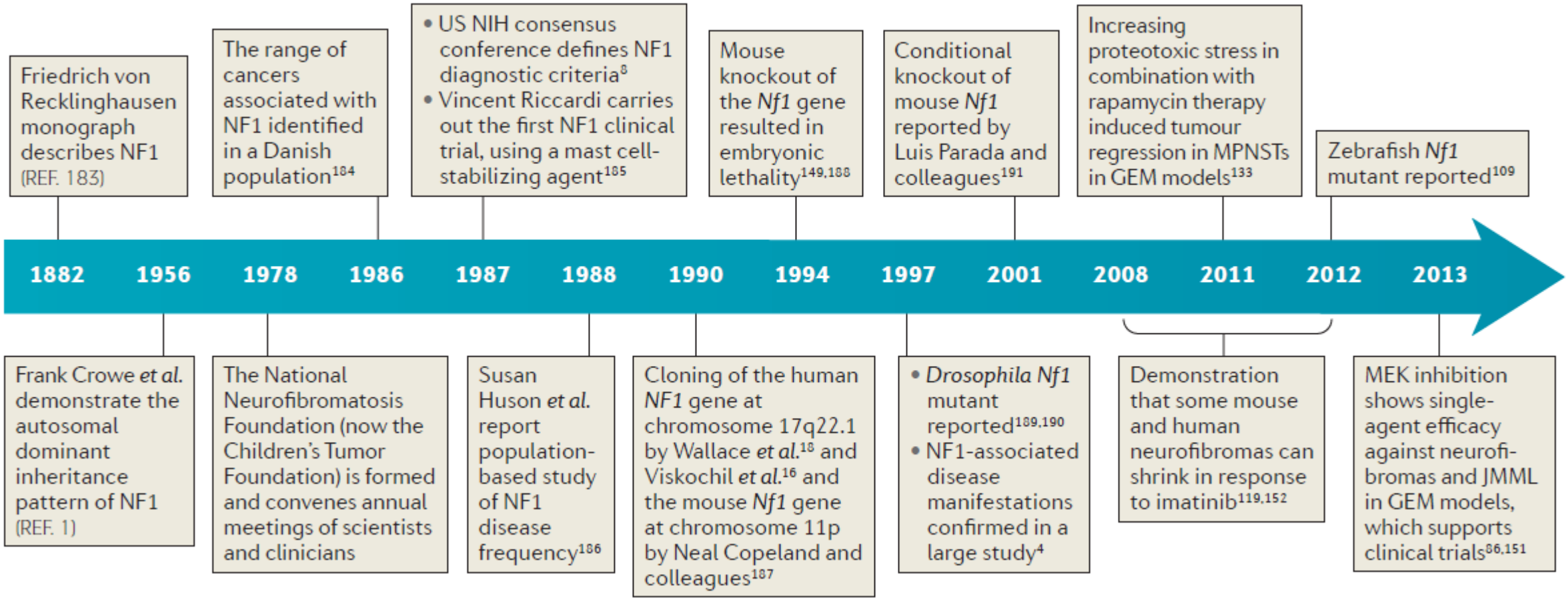

Ratner et al. Nature Reviews Cancer. 2015.

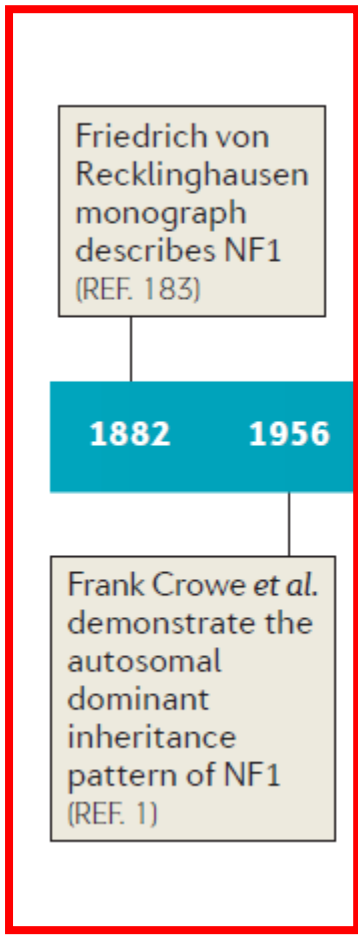

- Friedrich Daniel von Recklinghausen published his landmark paper (in German) *On the Multiple Fibromas of the Skin and Their Relationship to the Multiple Neuromas* in 1882.
- In 1956 Crowe, Schull, & Neel published a milestone manuscript detailing the numerous manifestations of this disorder and demonstrated the autosomal dominant inheritance pattern.
- Penetrance approaches 100% by age 20
- Expressivity is highly *variable*, even among family members with the same mutation
  - important for genetic counseling, because an individual with mild clinical findings can have a child with a more severe phenotype, or vice versa

Ratner et al. Nature Reviews Cancer. 2015.

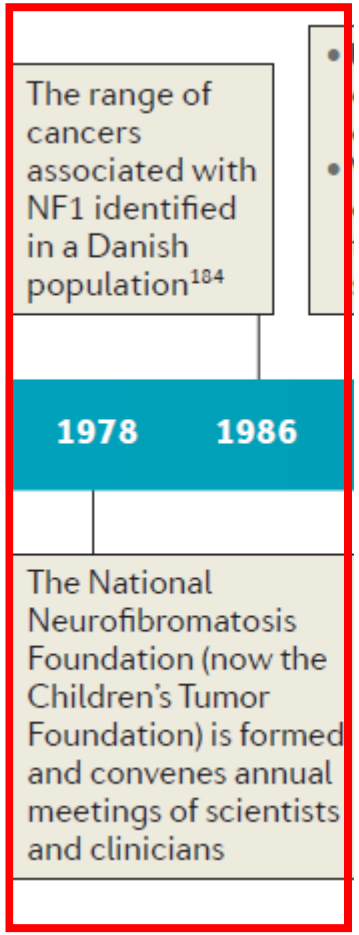

	Lifetime risk
Glioma of the optic pathway	15–20%
Other brain tumour	More than fivefold increase
Malignant peripheral nerve-sheath tumour	8–13%
Gastrointestinal stromal tumour	4–25%
Breast cancer	About fivefold increase
Leukaemia	About sevenfold increase
Phaeochromocytoma	0·1–5·7%
Duodenal carcinoid tumour	1%
Rhabdomyosarcoma	1·4–6%

Table: **Lifetime risk of different tumours in children and adults with neurofibromatosis type 1**

Ratner et al. Nature Reviews Cancer. 2015.

Hirbe et al. Lancet Neurology. 2014

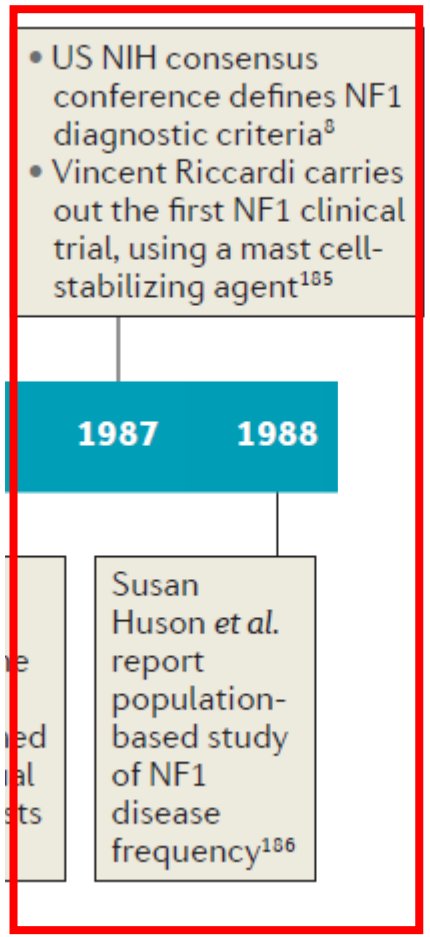

Panel: NIH consensus criteria[14] for diagnosis of neurofibromatosis type 1

Two or more of the following clinical features are sufficient to establish a diagnosis of neurofibromatosis type 1:

- Six or more café-au-lait macules (>0·5 cm at largest diameter in a prepubertal child or >1·5 cm in post-pubertal individuals)
- Axillary freckling or freckling in inguinal regions
- Two or more neurofibromas of any type or one or more plexiform neurofibromas
- Two or more Lisch nodules (iris hamartomas)
- A distinctive osseous lesion (sphenoid wing dysplasia, long-bone dysplasia)
- An optic pathway glioma
- A first-degree relative with neurofibromatosis type 1 diagnosed by the above criteria

NIH=National Institutes of Health.

Ratner et al. Nature Reviews Cancer. 2015.

Hirbe et al. Lancet Neurology. 2014

NF1: Diagnosis

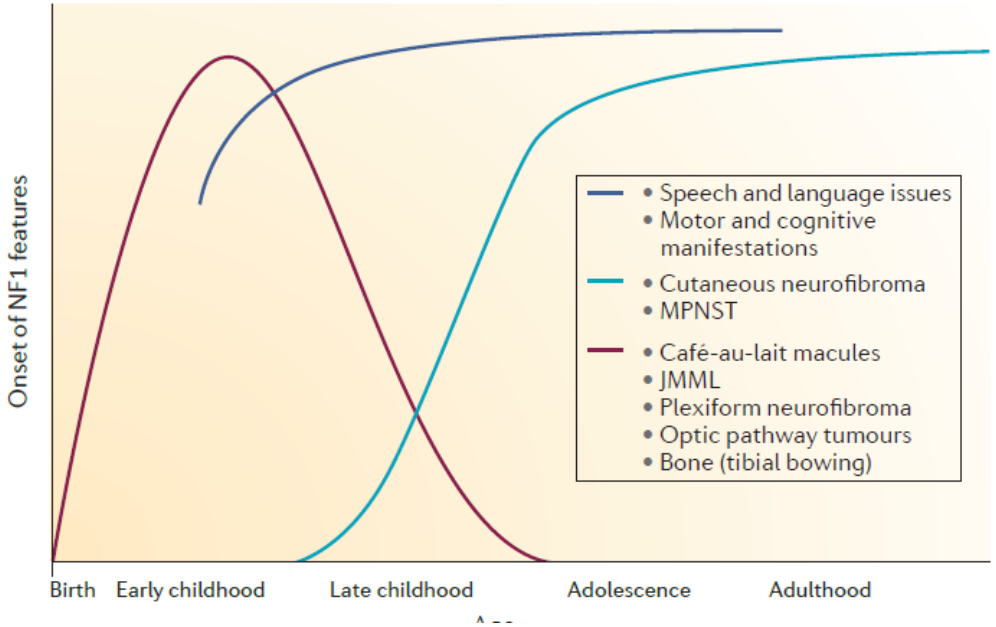

Ratner et al. Nature Reviews Cancer. 2015.

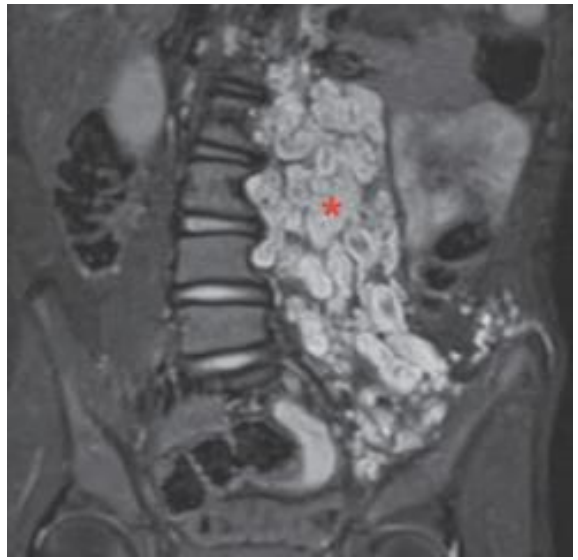

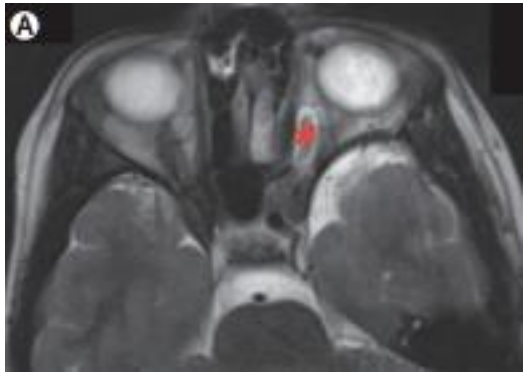

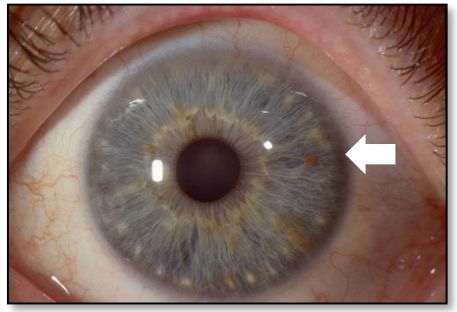

Hirbe et al. Lancet Neurology. 2014

NF1

rries
nical
ell-

Mouse knockout of the *Nf1* gene resulted in embryonic lethality[149,188]

1990 **1994**

Cloning of the human *NF1* gene at chromosome 17q22.1 by Wallace *et al.*[18] and Viskochil *et al.*[16] and the mouse *Nf1* gene at chromosome 11p by Neal Copeland and colleagues[187]

- Genetic linkage analysis: Chromosome 17
- Multipoint mapping: 17q11.2
- 2 patients with NF1 with balanced translocations (1 and 17, 17 and 22)
- Cloning efforts focused on the area between the breakpoints
  - NF1LT: interrupted in both translocations and found mutated in another patient

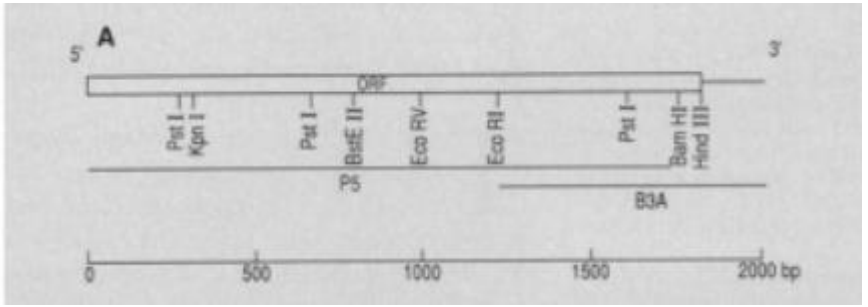

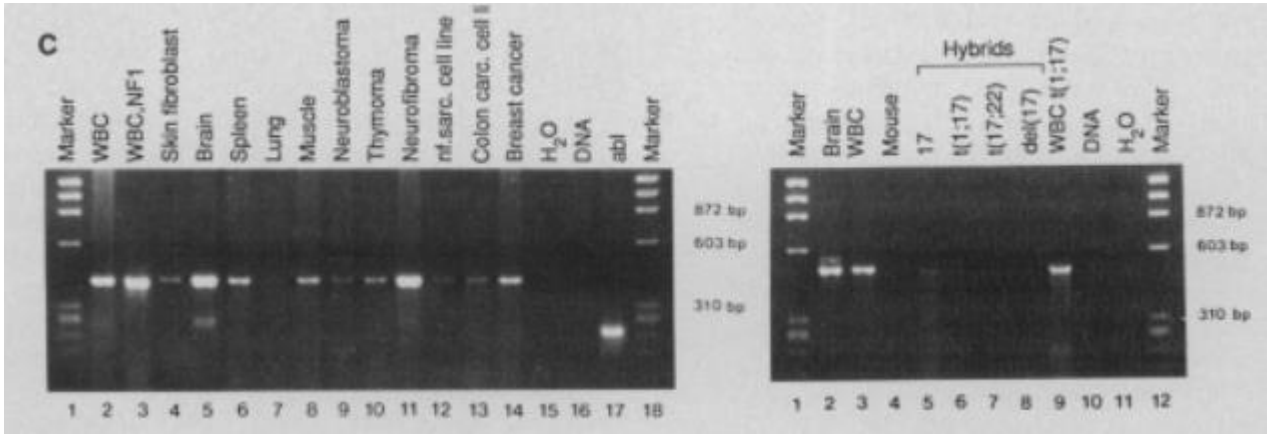

Ratner et al. Nature Reviews Cancer. 2015.

Wallace et al. Science. 1991.

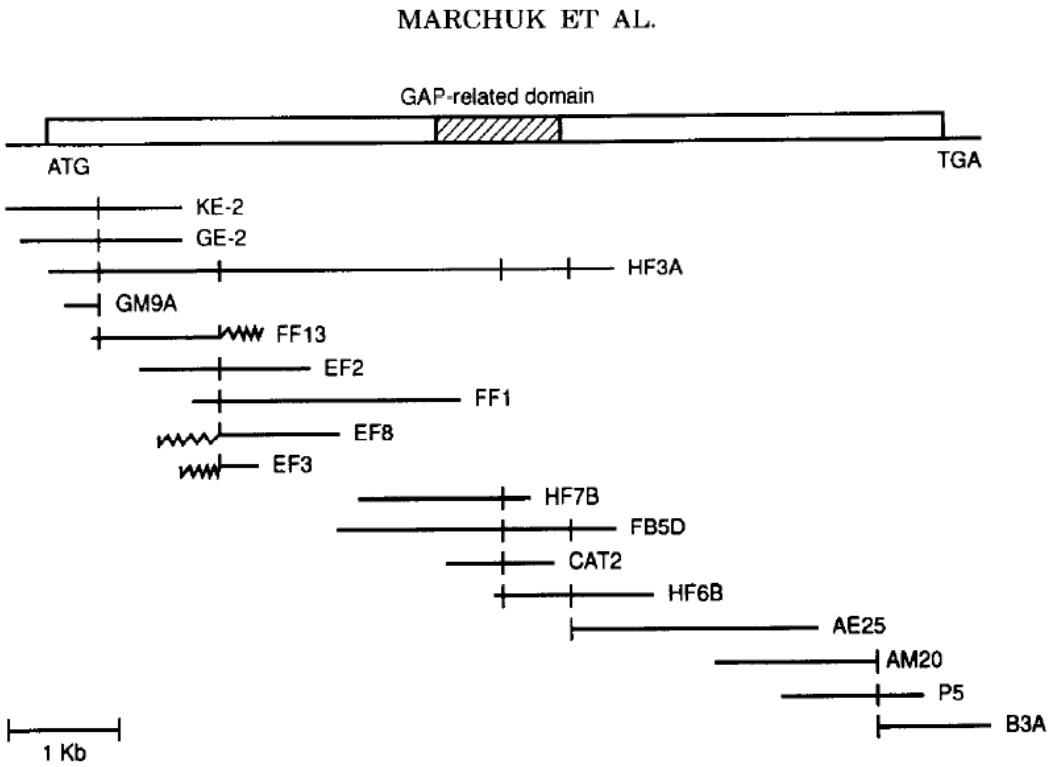

Marchuk et al. Genomics. 1991.

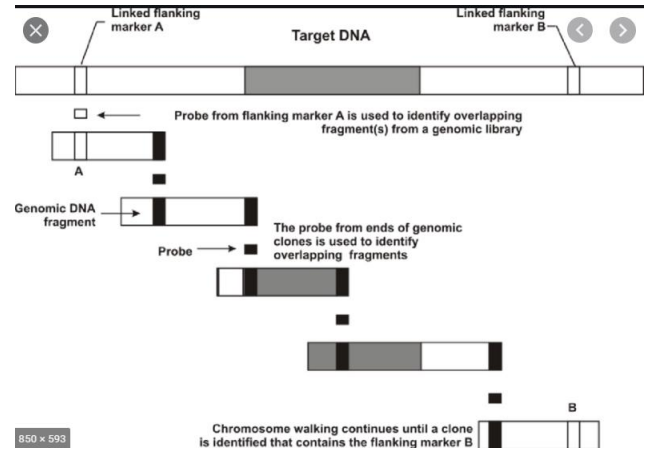

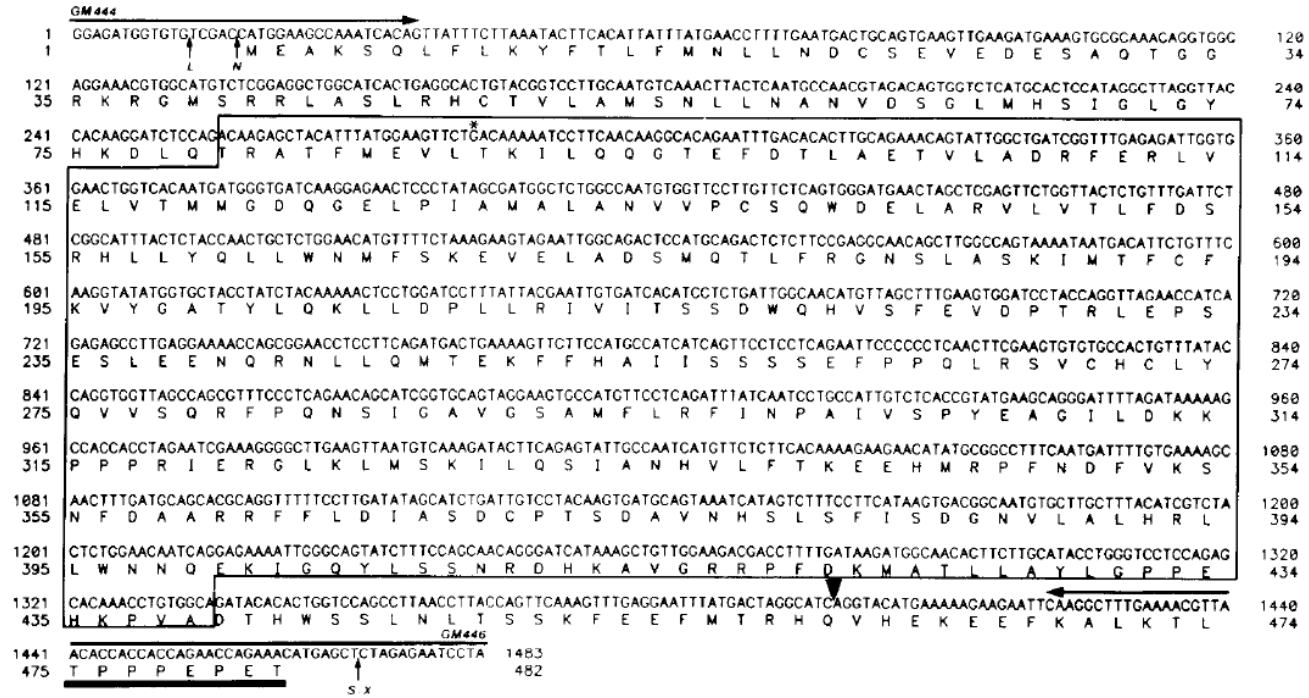

Figure 1. Nucleotide Sequence and Predicted Amino Acid Sequence of the GAP-Related Domain of NF1

Martin et al. Cell. 1990.

Aberrant regulation of *ras* proteins in malignant tumour cells from type 1 neurofibromatosis patients

Tanya N. Basu*, David H. Gutmann†, Jonathan A. Fletcher‡, Thomas W. Glover§, Francis S. Collins† & Julian Downward*||

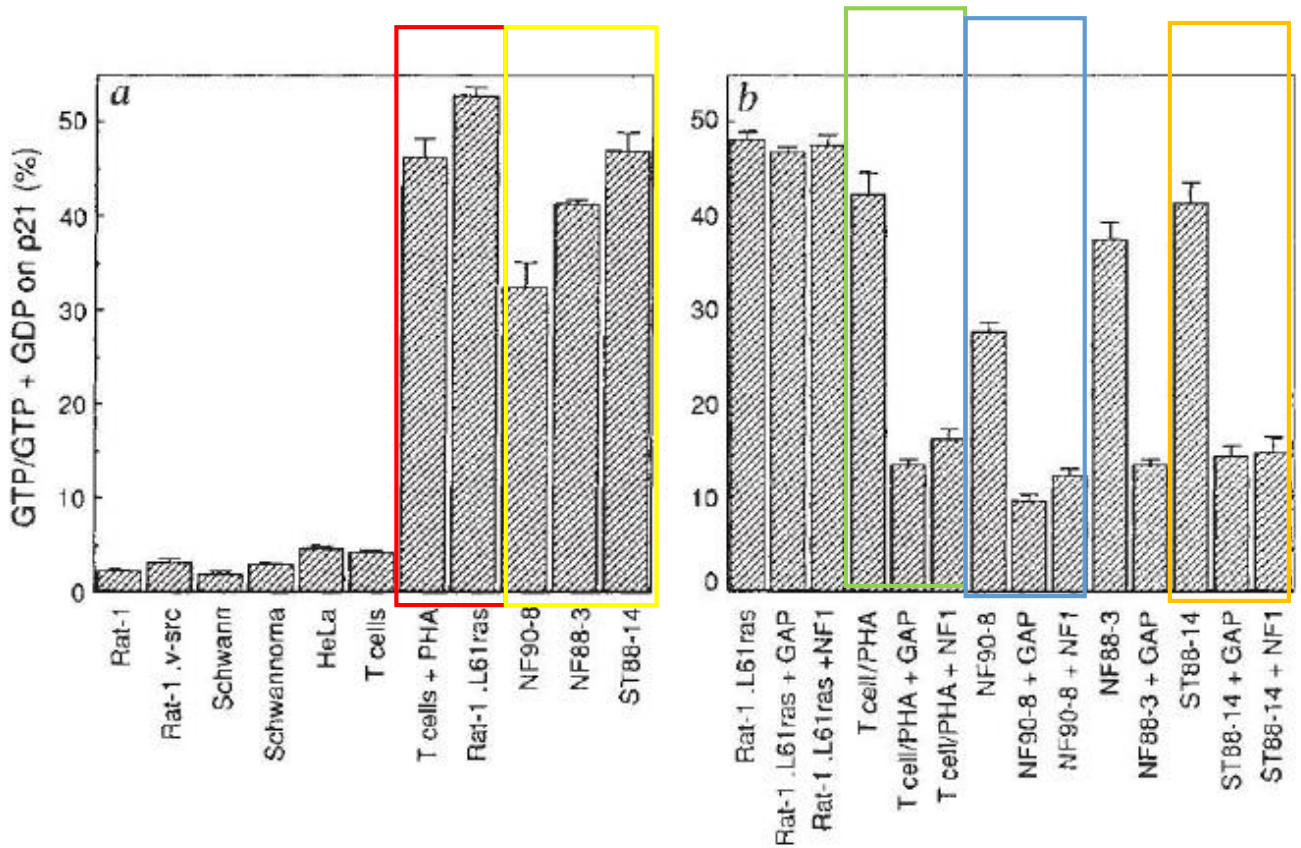

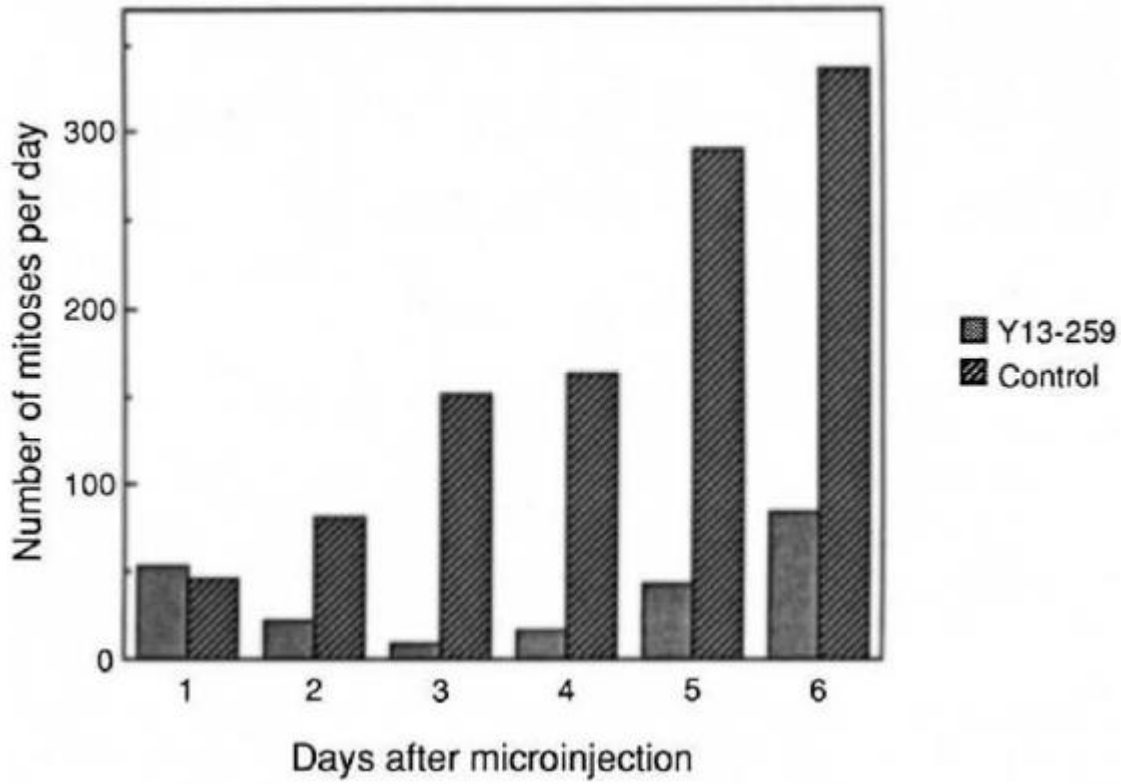

Basu et al. Nature. 1992

Neurofibromin Signaling

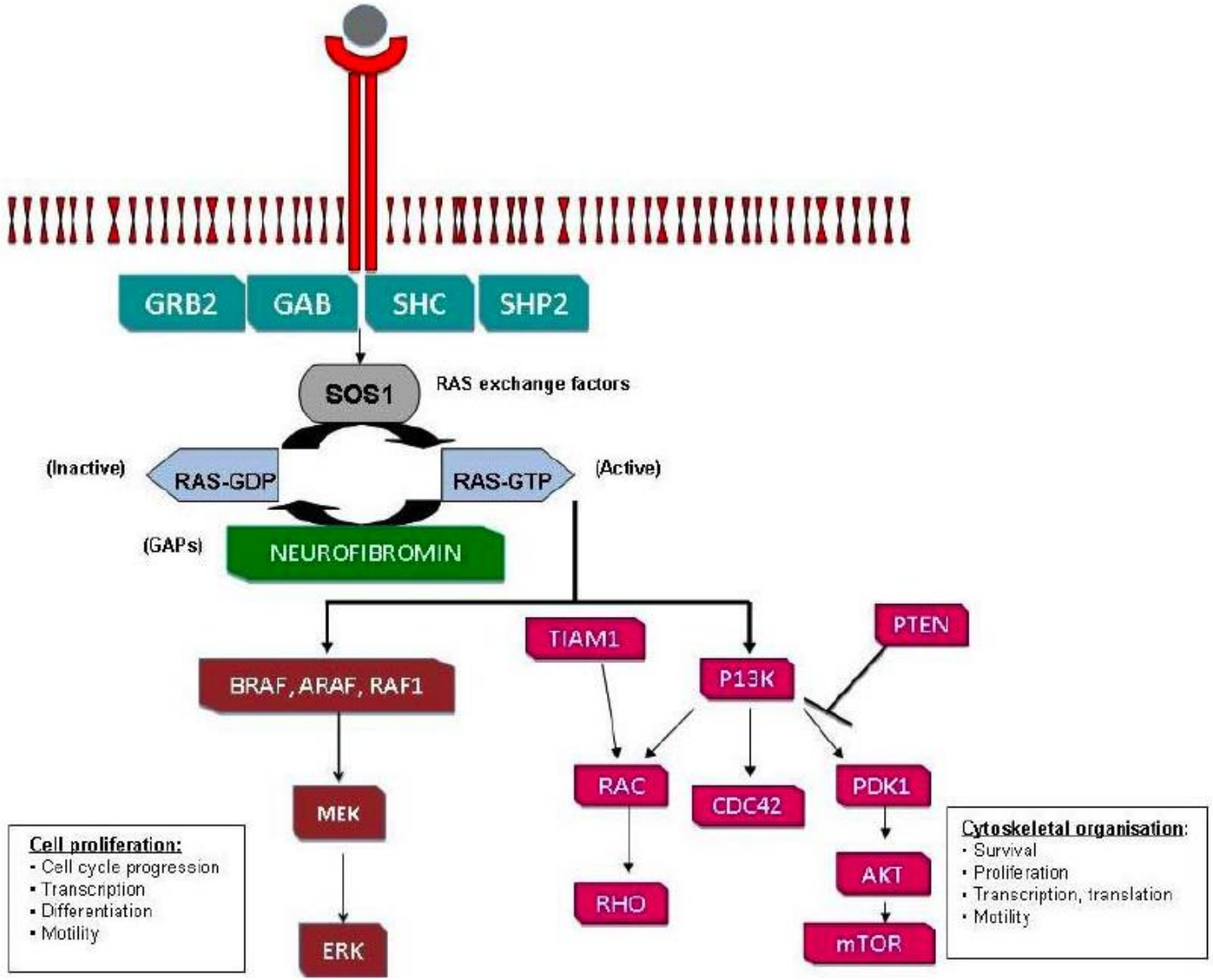

[Frontiers in Bioscience 16, 937-951, January 1, 2011]

Proc. Natl. Acad. Sci. USA
Vol. 88, pp. 9658–9662, November 1991
Biochemistry

Identification of the neurofibromatosis type 1 gene product

(protein/antibodies/GTPase-activating protein)

DAVID H. GUTMANN, DEBORAH L. WOOD, AND FRANCIS S. COLLINS*

Departments of Internal Medicine and Human Genetics and The Howard Hughes Medical Institute, The University of Michigan, Ann Arbor, MI 48109-0650

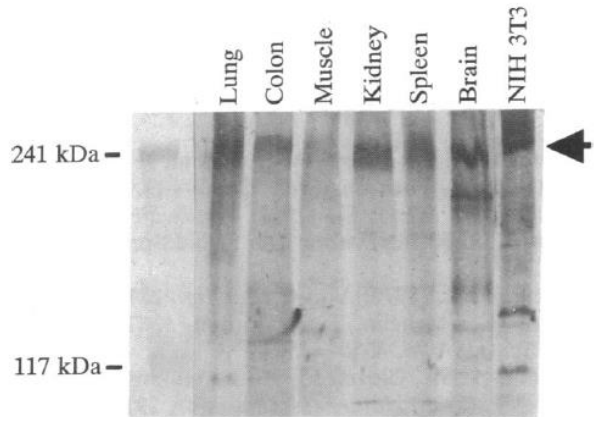

Cell, Vol. 63, 843–849, November 16, 1990, Copyright © 1990 by Cell Press

The GAP-Related Domain of the Neurofibromatosis Type 1 Gene Product Interacts with *ras* p21

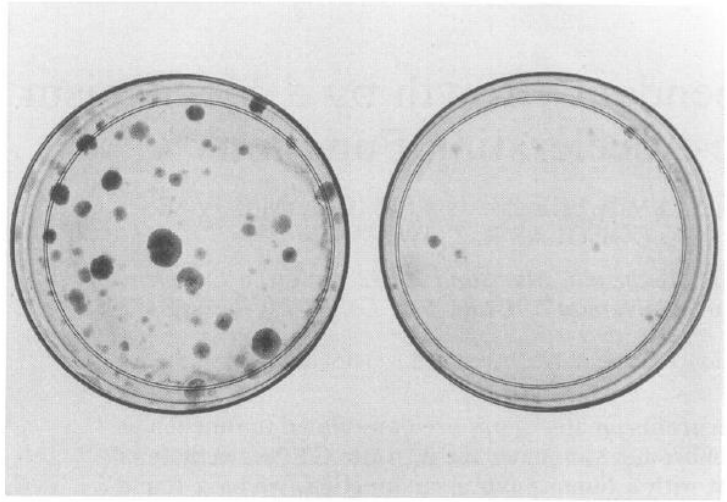

FIG. 1. *NF1* inhibits NIH 3T3 cell colony formation. NIH 3T3 cells were transfected with the control pGV16 vector (15) containing the neomycin resistance gene (left) or the full-length *NF1* cDNA (right). After 16 days of selection in Geneticin, the plates were stained with methylene blue-carbon fuchsia.

THE JOURNAL OF BIOLOGICAL CHEMISTRY

Vol. 268, No. 30, Issue of October 25, pp. 22331–22337, 1993
Printed in U.S.A.

The GTPase-activating NF1 Fragment of 91 Amino Acids Reverses v-Ha-Ras-induced Malignant Phenotype*

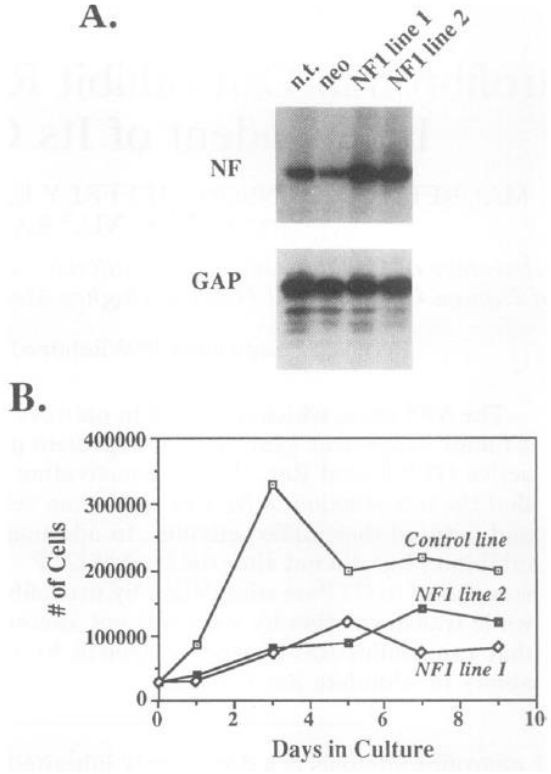

Johnson et al. Molecular and Cellular Biology. 1994.

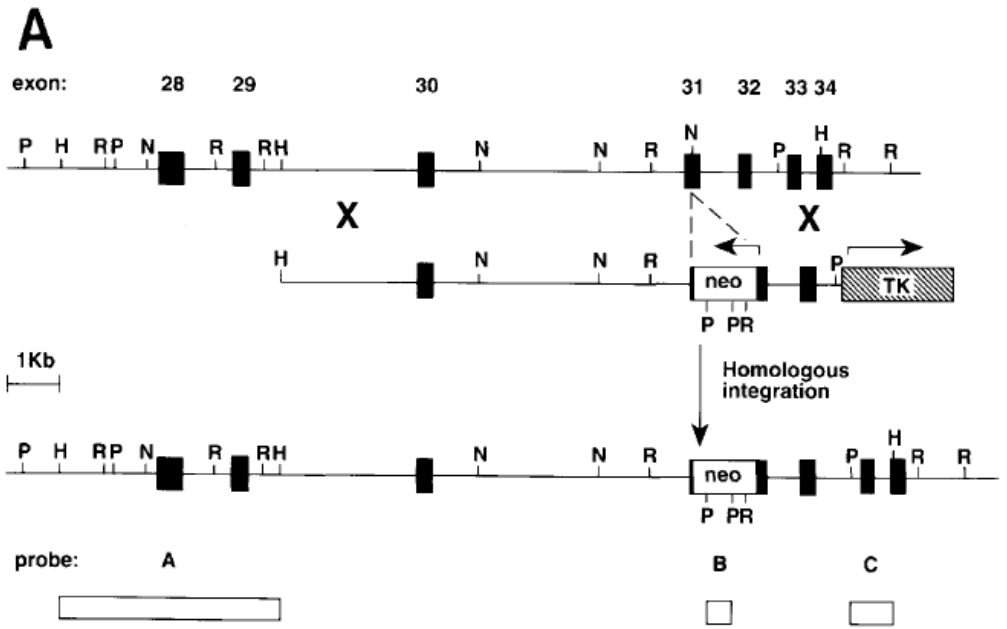

Predicted fragment sizes

Allele	Probe A *Pst* I	Probe B *Pst* I	Probe C *Eco* RI
Wild-type (Kb)	11.8 1.6	-	3.2
Mutant (Kb)	11.0 1.6	11.0	2.6

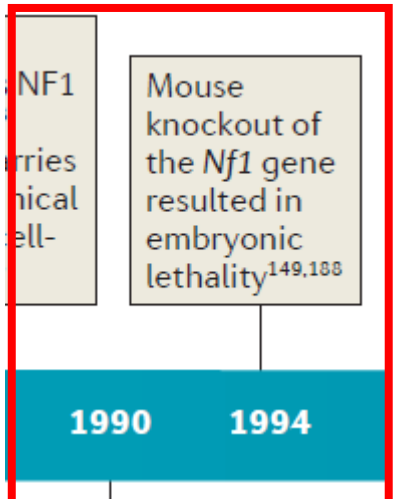

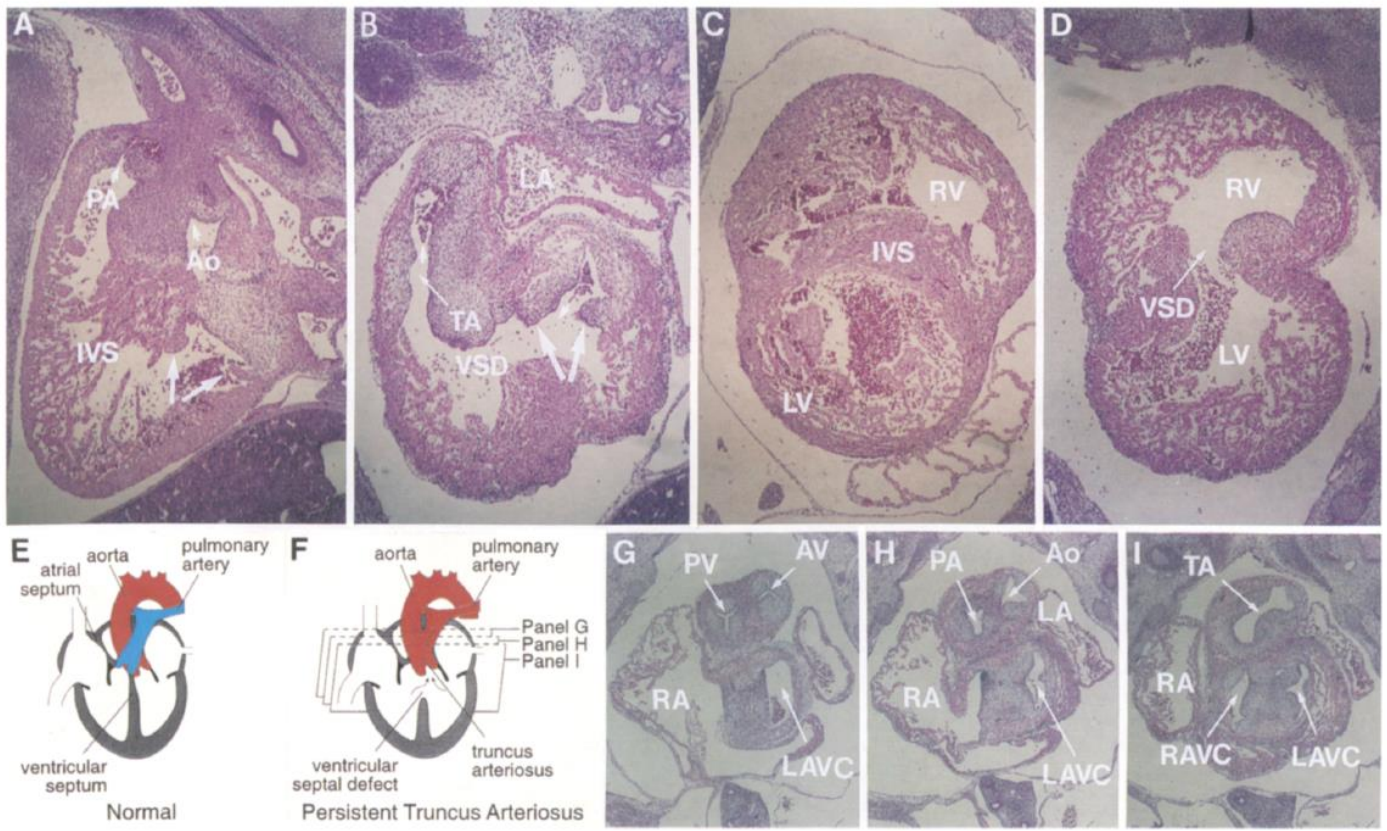

Brannan et al. Genes and Development. 1994.

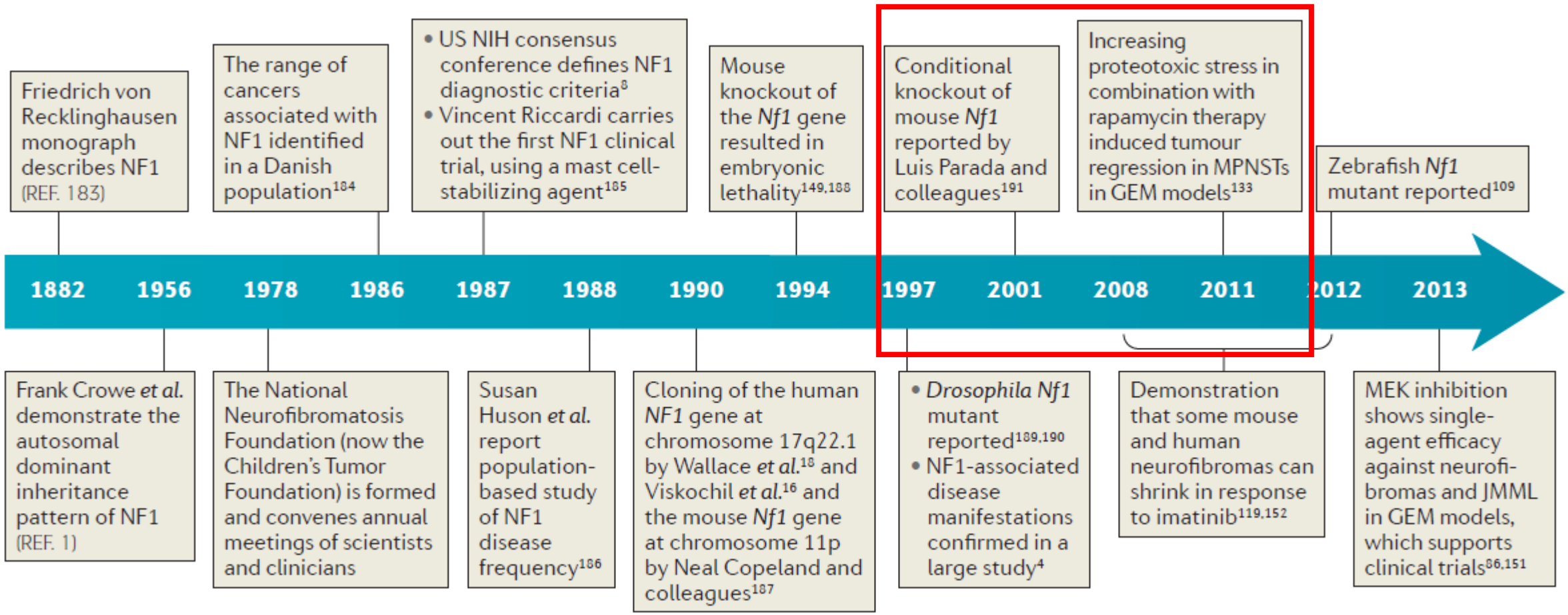

Ratner et al. Nature Reviews Cancer. 2015.

Mouse Models of Tumor Development in Neurofibromatosis Type 1

Karen Cichowski,[1]* T. Shane Shih,[1,2]* Earlene Schmitt,[1,3] Sabrina Santiago,[1] Karlyne Reilly,[1] Margaret E. McLaughlin,[4] Roderick T. Bronson,[5] Tyler Jacks[1,6]†

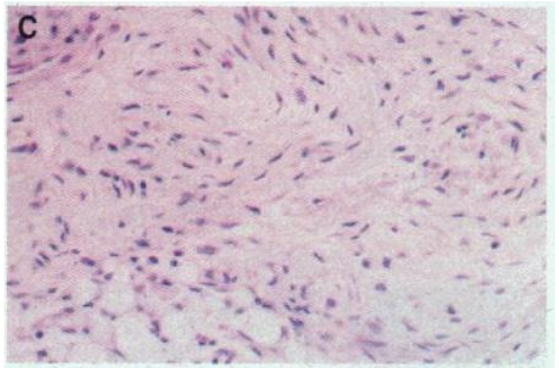

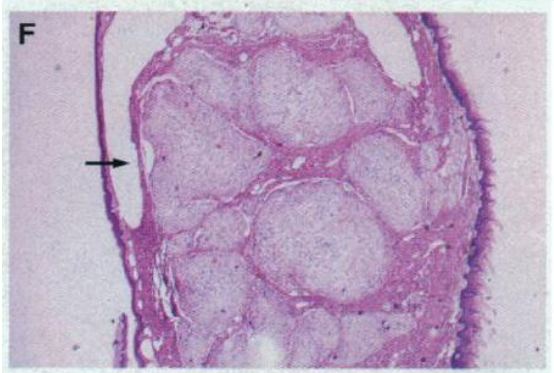

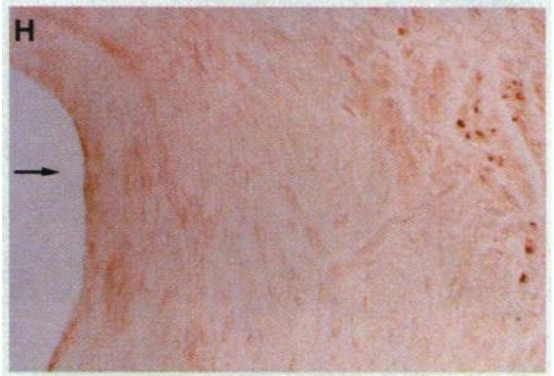

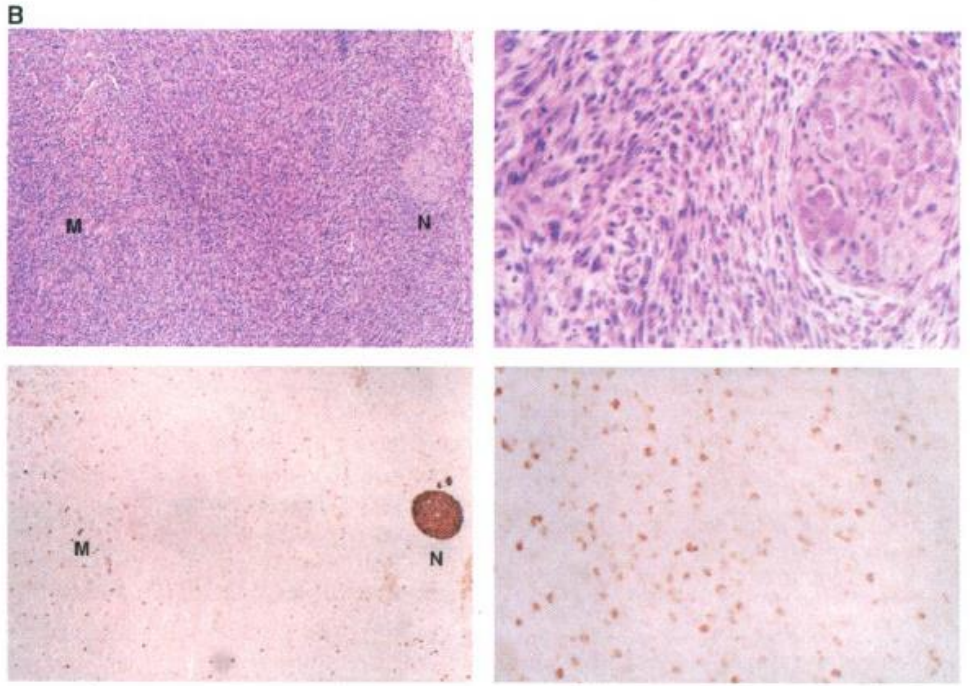

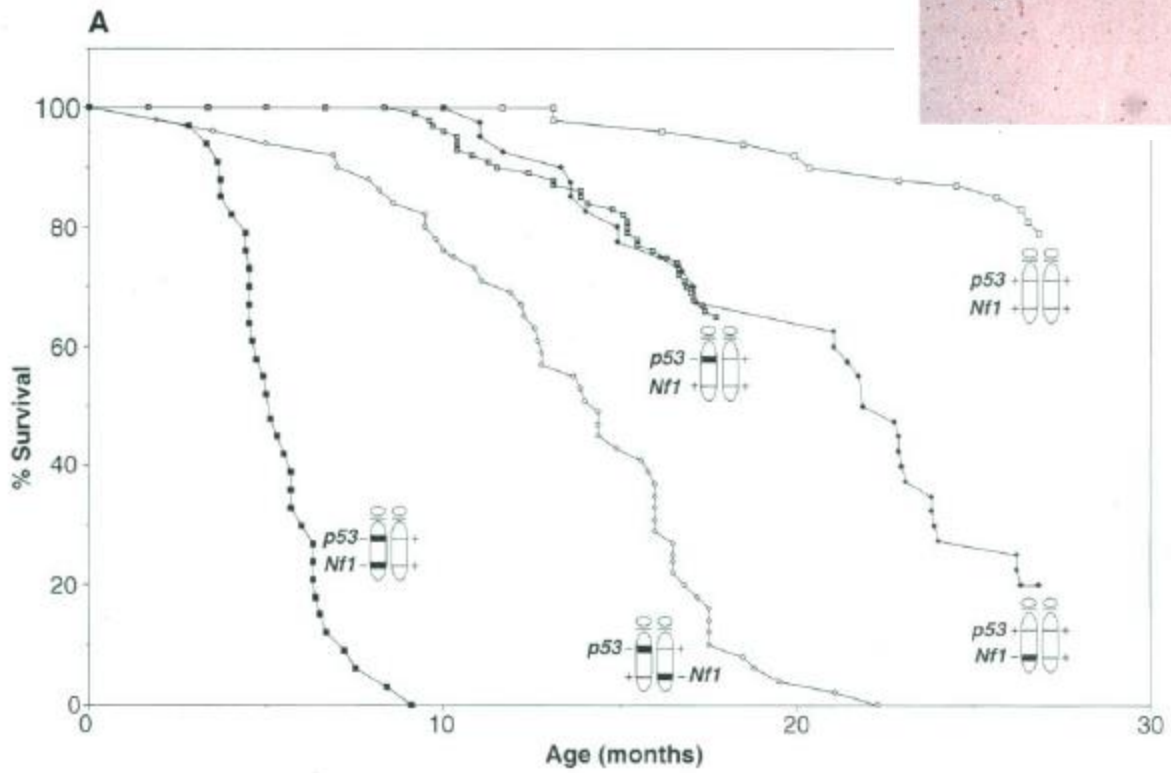

Cichowski et al. Science. 1999.

Ablation of NF1 function in neurons induces abnormal development of cerebral cortex and reactive gliosis in the brain

Yuan Zhu,[1] Mario I. Romero,[1] Pritam Ghosh,[1] Zhengyi Ye,[2] Patrick Charnay,[3] Elizabeth J. Rushing,[4] Jamey D. Marth,[2] and Luis F. Parada[1,5]

Optic Nerve Glioma in Mice Requires Astrocyte *Nf1* Gene Inactivation and *Nf1* Brain Heterozygosity

M. Livia Bajenaru,[1] M. Rosario Hernandez,[2] Arie Perry,[3] Yuan Zhu,[6] Luis F. Parada,[6] Joel R. Garbow,[4,5] and David H. Gutmann[1]

Departments of [1]Neurology, [2]Ophthalmology, [3]Pathology, [4]Radiology, and [5]Chemistry, Washington University School of Medicine, St. Louis, Missouri, and [6]Center for Developmental Biology and Kent Waldrep Foundation Center for Basic Research on Nerve Growth and Regeneration, University of Texas Southwestern Medical Center, Dallas, Texas

Cancer Cell
Article

Induction of Abnormal Proliferation by Nonmyelinating Schwann Cells Triggers Neurofibroma Formation

Huarui Zheng,[1,5] Lou Chang,[1,5] Neha Patel,[1,2] Jiong Yang,[1] Lori Lowe,[3] Dennis K. Burns,[4] and Yuan Zhu[1,*]

Periostin-Cre X *Nf1*$^{flox/flox}$

Periostin-Cre; *Nf1*$^{flox/flox}$

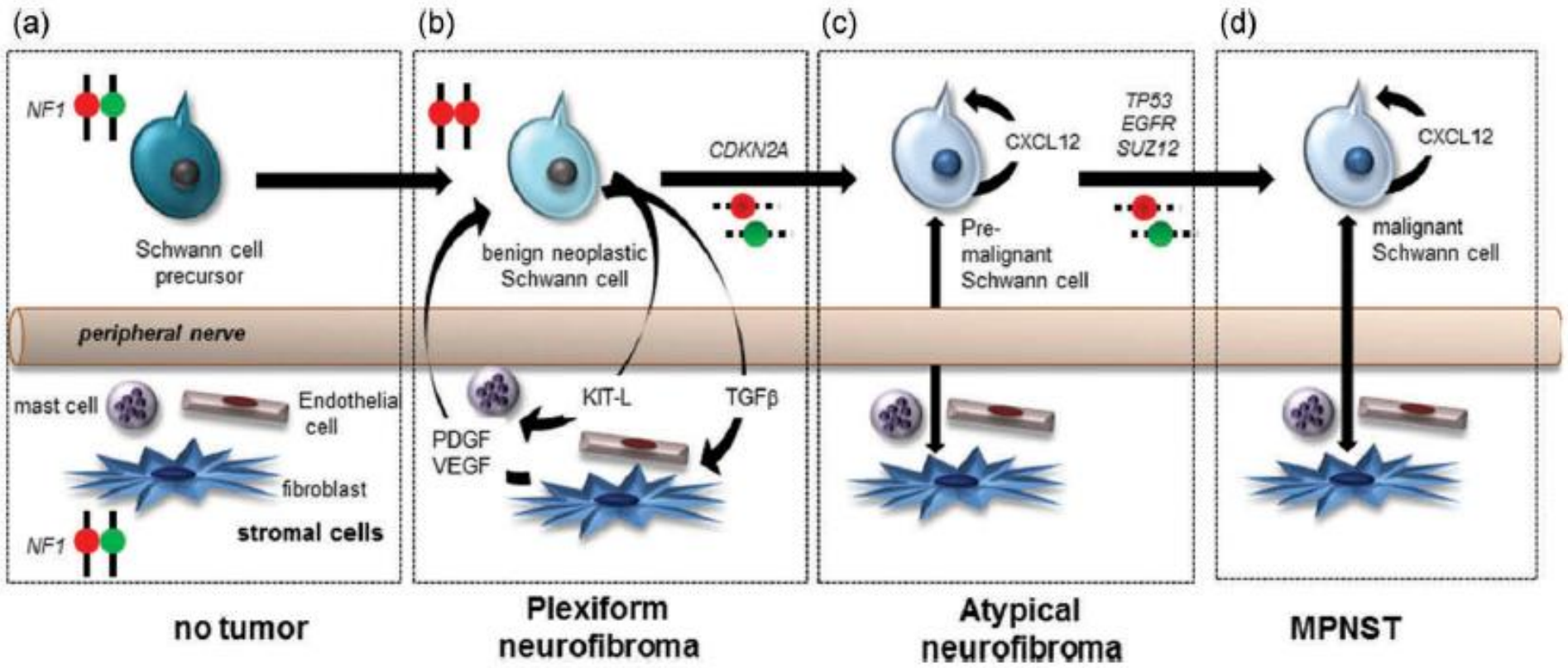

Hirbe et al. Expert Opinion On Orphan Drugs. 2017

How will we advance treatment for peripheral nervous system tumors?

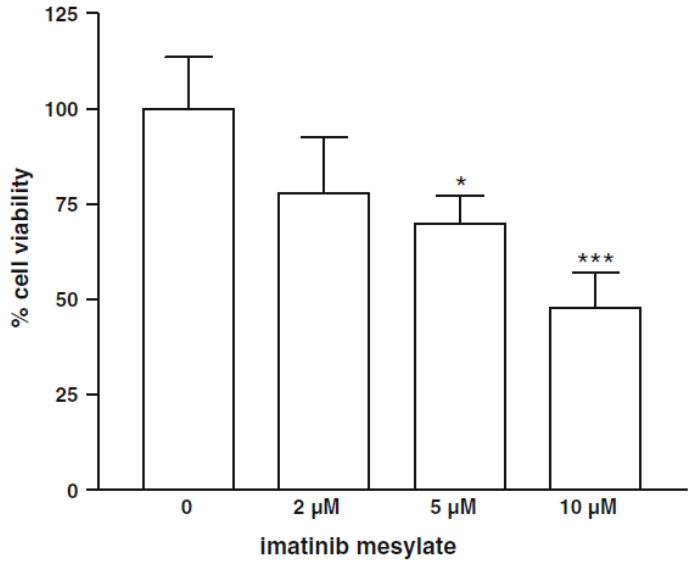

Fig. 2 Imatinib mesylate treatment reduced viability of PNF Schwann cells. Primary Schwann cell cultures derived from PNF were treated with imatinib mesylate at various concentrations for 28 days. Data was normalized from the absorbance values of untreated cells and data are expressed as percentage cell viability. Significant reduction in cell viability was detected for 5 and 10 μM imatinib mesylate treatment (*$P < 0.05$ and ***$P < 0.001$, respectively) when compared with untreated cells

Demestre et al. J Neurooncol. 2010.

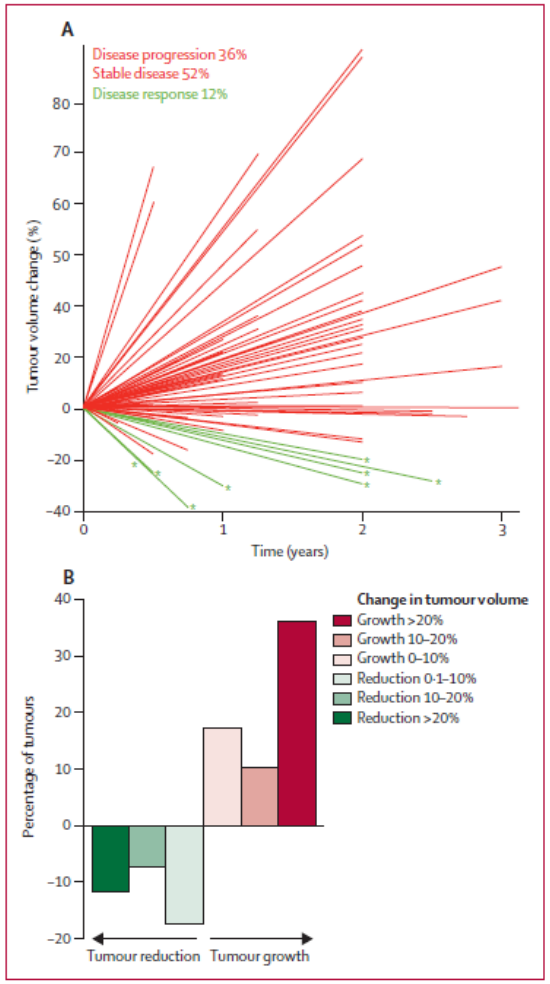

Figure 2: **Change in volume of plexiform neurofibromas in patients with NF1**
(A) Green lines with asterisks represent tumours that decreased in volume over time as evidenced by MRI measurements; red lines represent growing tumours including those not decreasing by ≥20% in volume. (B) Relative percentage of tumours in patients given imatinib mesylate, expressed by percentage change in tumour volume.

Robertson et al. Lancet Oncol. 2012.

- Imatinib mesylate occupies the ATP binding pocket of the c KIT kinase domain
- This prevents substrate phosphorylation and signaling
- A lack of signaling inhibits proliferation and survival

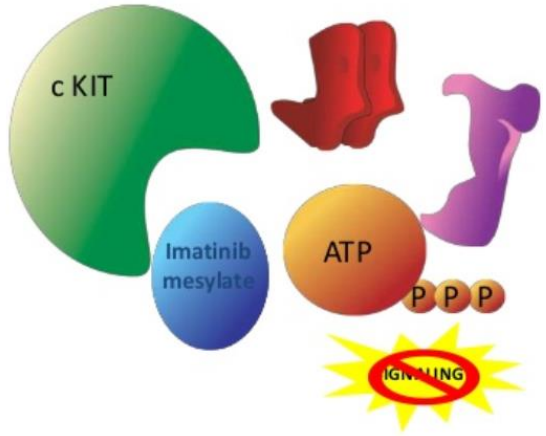

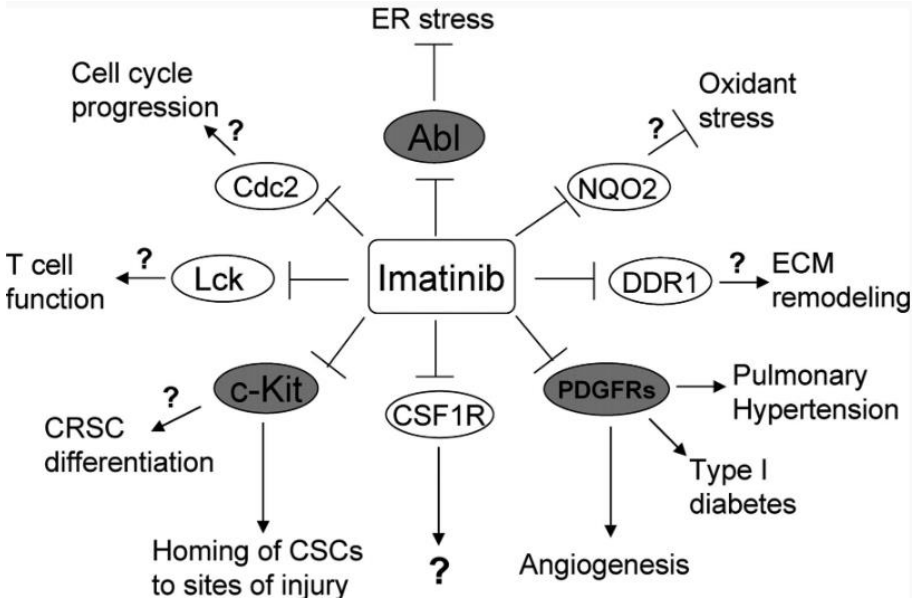

Cheng et al. Circulation Research 2010.

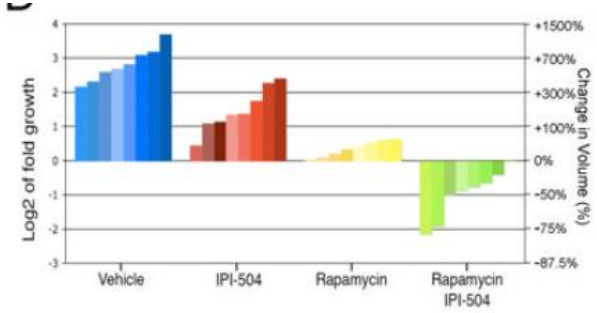

	Vehicle	IPI-504	Rap	Rap IPI-504
Mean (Log2 fold)	2.83	1.49	0.37	-0.96 (45% regression)
Standard deviation	0.50	0.65	0.24	0.73
Shapiro-Wilk p-value	0.92	0.72	0.50	0.44
t-test (separate var)	4.4 10⁻⁴		0.001	

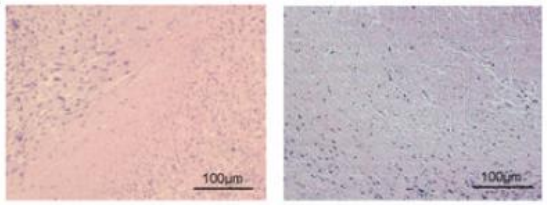

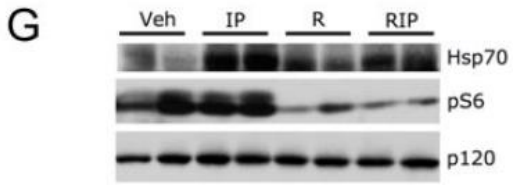

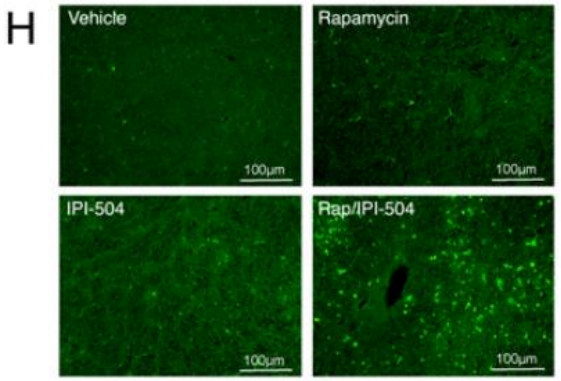

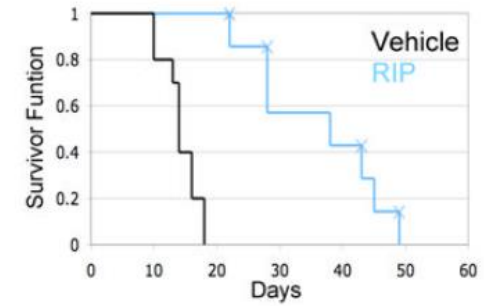

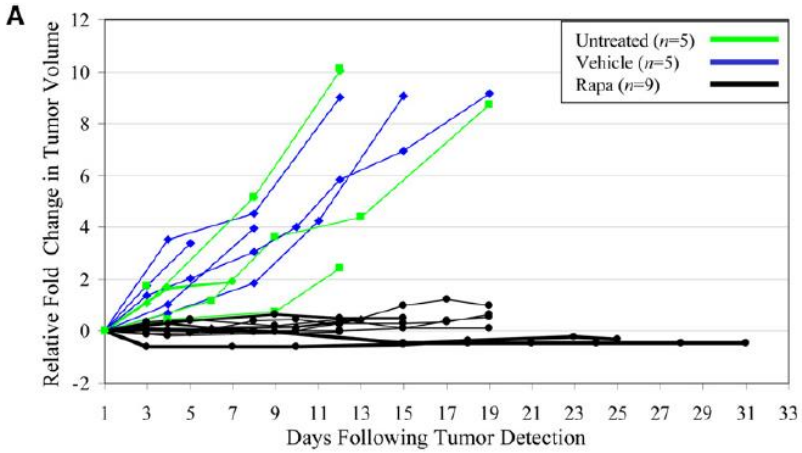

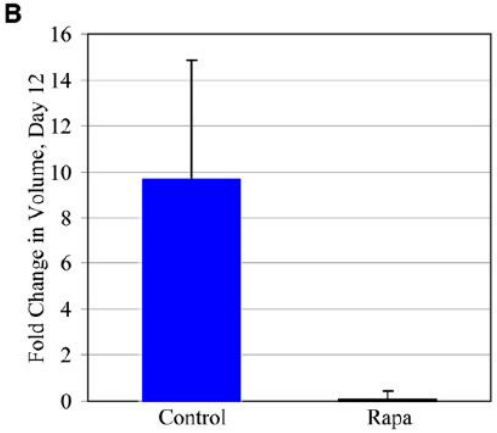

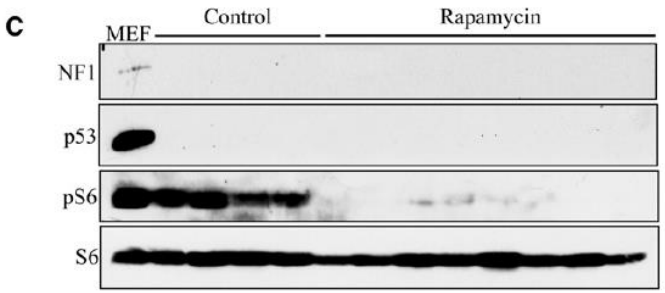

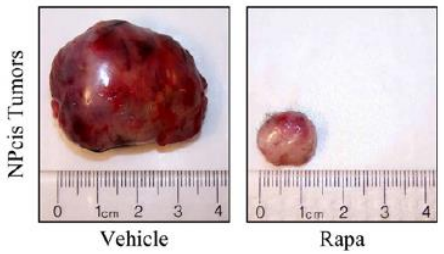

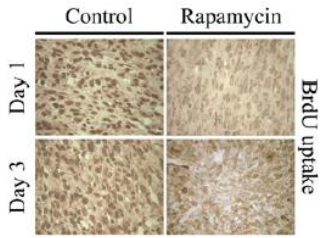

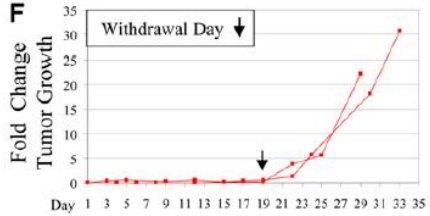

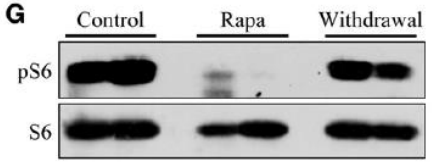

DeRaedt et al. Cacer Cell. 2011.

Johannessen et al. Current Biology 2008.

Where are we today?

Table 1. Demographic, Clinical, and Baseline Disease Characteristics.

Characteristic	Value
Number of patients enrolled	24
Median age at enrollment (range) — yr	10.9 (3.0–18.5)
Sex — no.	
Male	13
Female	11
Median performance status score (range)*	90 (70–100)
No. of previous medical interventions for treatment of plexiform neurofibroma	41
No. of patients who had previous medical interventions	19
Median no. of previous medical interventions per patient (range)	2 (1–6)
No. of previous plexiform neurofibroma debulking surgeries	25
No. of patients who underwent previous debulking surgeries	11
Median no. of previous debulking surgeries per patient (range)	1 (1–6)
Predominant target location of plexiform neurofibroma — no.	
Face	4
Both head and neck	1
Both neck and chest	6
Trunk	4
Both trunk and extremity (upper or lower)	8
Whole body	1
Median target plexiform neurofibroma volume (range) — ml	1205 (29–8744)
Progression status of target plexiform neurofibroma at enrollment — no. (%)	
Progressive	9 (38)
Nonprogressive	8 (33)
Insufficient information	7 (29)
Documented plexiform neurofibroma–related complication at baseline — no. (%)	21 (88)
Disfigurement	18 (75)
Pain	13 (54)
Motor dysfunction	9 (38)
Vision loss	1 (4)

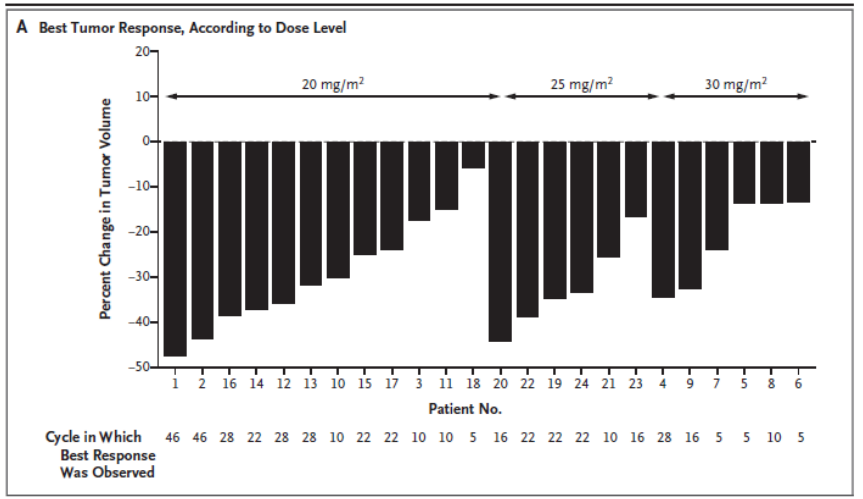

Dombi et al. NEJM.2016

No Advances in Therapy

- Despite increased knowledge regarding the biology of MPNSTs, no clinical trial based on current preclinical models has been successful.

Therapy	Molecular Targets	No. of MPNSTs	Study Design and Population	Response	Reference
Erlotinib	EGFR	20	Phase II study in MPNST	No objective responses, 1 stable disease	72
Sorafenib	VEGFR, RAF, PDGFR	12	Phase II study in soft tissue sarcomas	No objective responses	73
Imatinib	C-KIT, PDGFR, VEGFR	7	Phase II study in 10 subtypes of sarcoma	No objective responses, 1 stable disease	74
Dasatinib	c-KIT, c-SRC	14	Phase II study in bone and soft tissue sarcomas	No objective responses	75
Alisertib	Aurora Kinase A	10	Phase II study in advanced sarcomas	No objective responses	76
Bevacizumab/RAD001	VEGF/mTOR	25	Phase II study in MPNST	2 stable disease, 1 partial response after 2 cycles that progressed after cycle 4	77, 78
Ganetespib/Sirolimus	HSP90/mTOR	20	Phase I/II study in MPNST	Not fully reported	79
Pexidartinib/Sirolimus	c-KIT, PDGFR, CSFR1/mTOR	6	Phase I study in MPNSTs, PVNS, and other sarcomas	5 stable disease	80

Summary of Genomic Studies

Study	year	study size	molecular studies	*NF1*	*SUZ12*	*EED*	*TP53*	*CDKN2A*	Notes
De Raedt, *et al.*[4]	2014	51 MPNST	targeted sequencing, aCGH	NR (clinically 100%)	32/51 (63%)	15/51 (29%)	NR	NR	all NF1 patients
Zhang, *et al.*[5]	2014	50 MPNST	WGS (5), WES (3), targeted sequencing (42)	31/50 (62%)	16/50 (32%)	1/50 (2%)	1/8 (13%)	1/8 (13%)	limited copy number analysis
Lee, *et al.*[6]	2014	52 MPNST	WES, SNP array, and RNAseq (15); targeted sequencing (37)	45/52 (87%)	25/52 (48%)	19/52 (37%)	22/52 (42%)	42/52 (81%)	
Sohier, *et al.*[7]	2017	8 MPNST	WES, aCGH (7)	8/8 (100%)	7/8 (88%)	2/8 (25%)	1/8 (13%)	5/8 (63%)	all NF1 patients
current study	2017	12 MPNST	WES, SNP array (7)	11/12 (92%)	5/12 (42%)	4/12 (33%)	6/12 (50%)	7/12 (58%)	

Brohl et al. Scientific Reports. 2017

Why are we failing to improve therapy?

- Current preclinical models don't encompass the full spectrum of genetic heterogeneity that is seen in MPNST
- Treatments may work better for one disease subtype, which is currently not captured using a single genetic model.

How can we improve therapy?

- Identify subtypes and test therapies based on subtypes
- Develop Models that encompass the heterogeneity

GeM Consortium

- We hypothesize that multi-omic characterization of a large tumor set, at high depth, and with comparison to annotated clinical data, will identify distinct tumor subsets and inform pre-clinical research.

- The secondary goal is to better understand the relationship between tumor heterogeneity at the genomic level with histological markers of tumor behavior through multi-omic profiling and extensive pathological characterization utilizing tissue microarrays for immunohistochemistry.

Overview

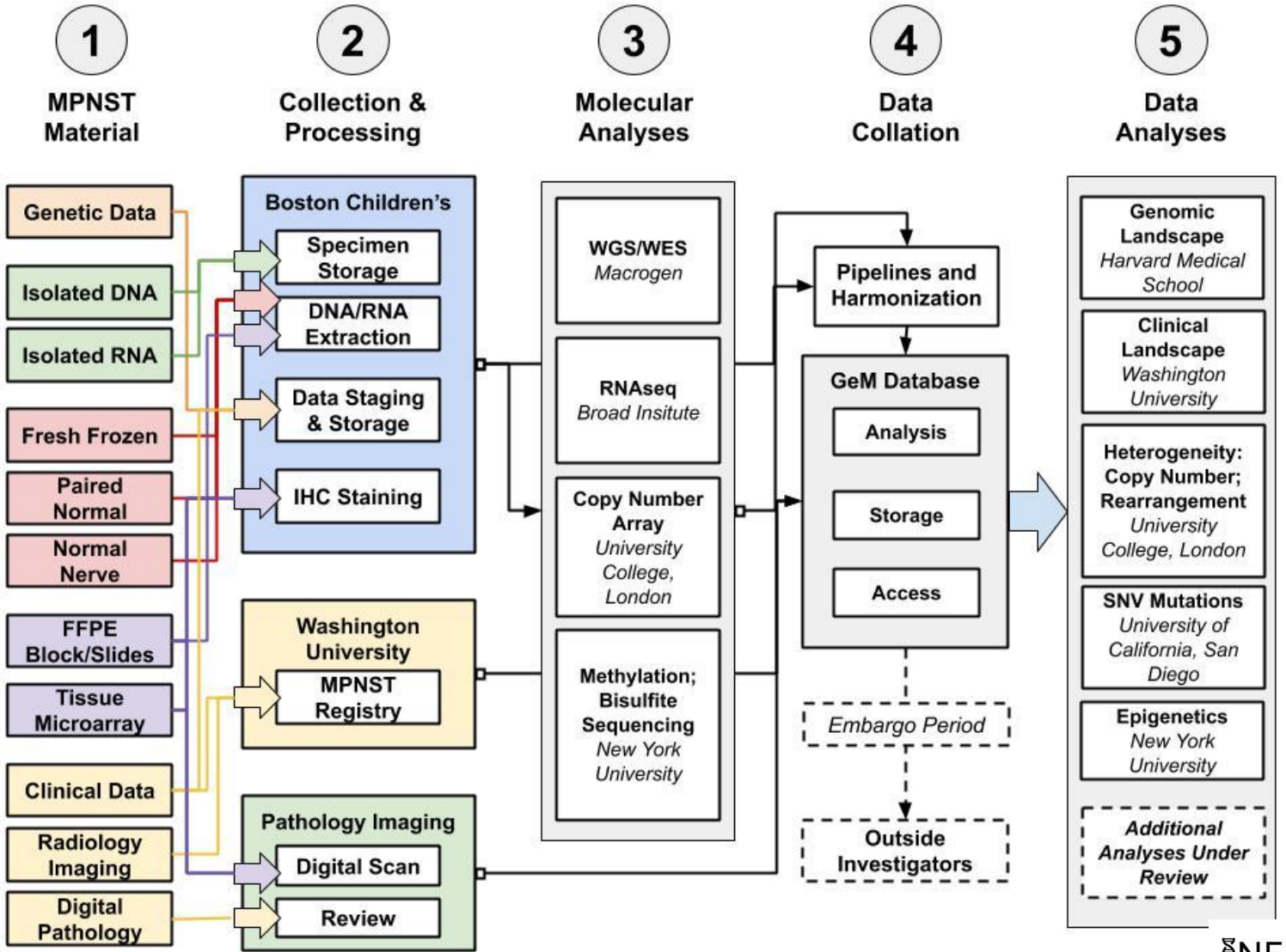

NF Research Initiative

Boston Children's Hospital Until every child is well

GeM Consortium Genomics of MPNST

Analysis Overview

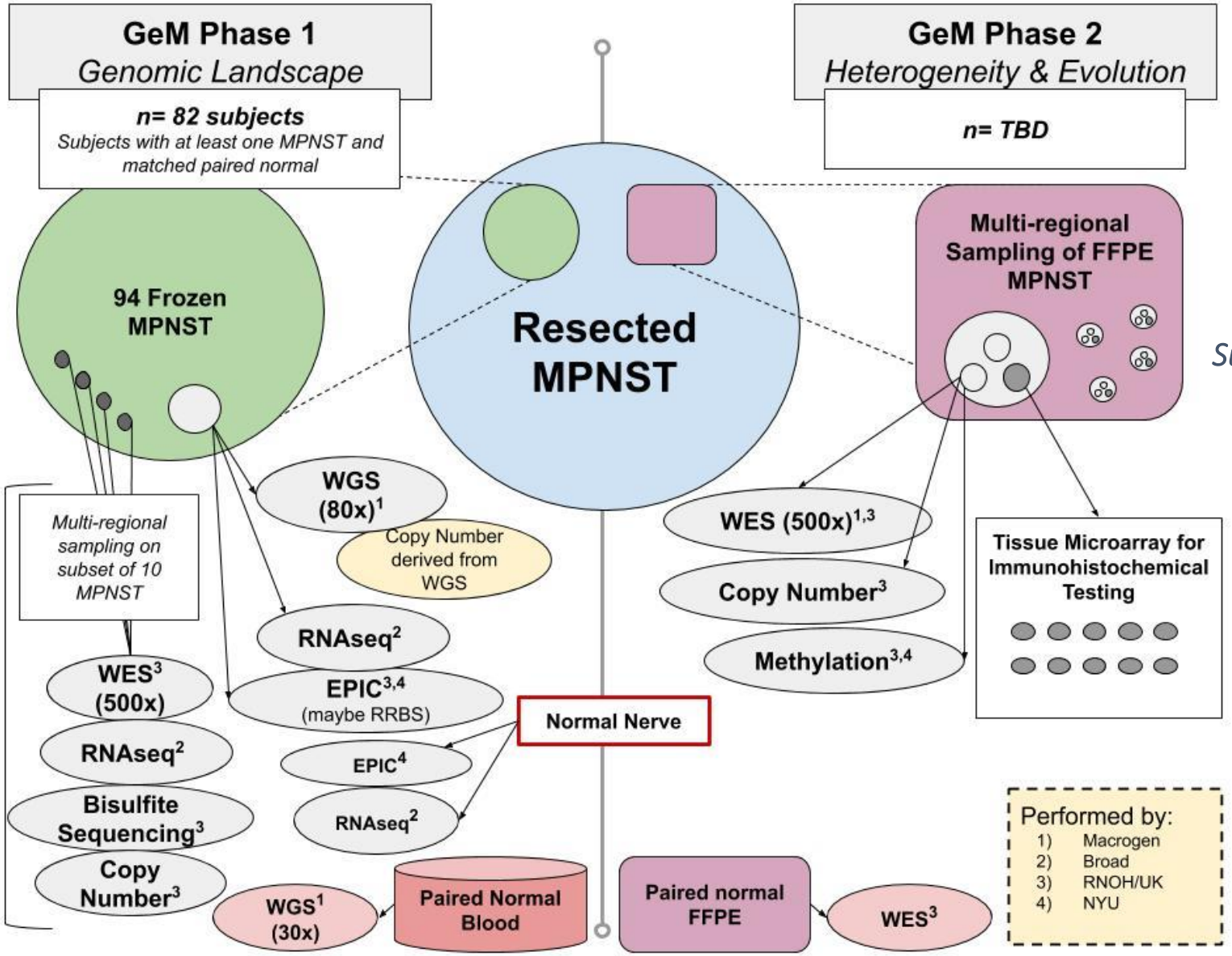

Summary data will be made available through cBioPortal.

cBioPortal FOR CANCER GENOMICS

NF Research Initiative

Boston Children's Hospital Until every child is well

GeM Consortium Genomics of MPNST

Development of a Preclinical NF1-MPNST Platform Suitable for Precision Oncology Drug Discovery and Evaluation

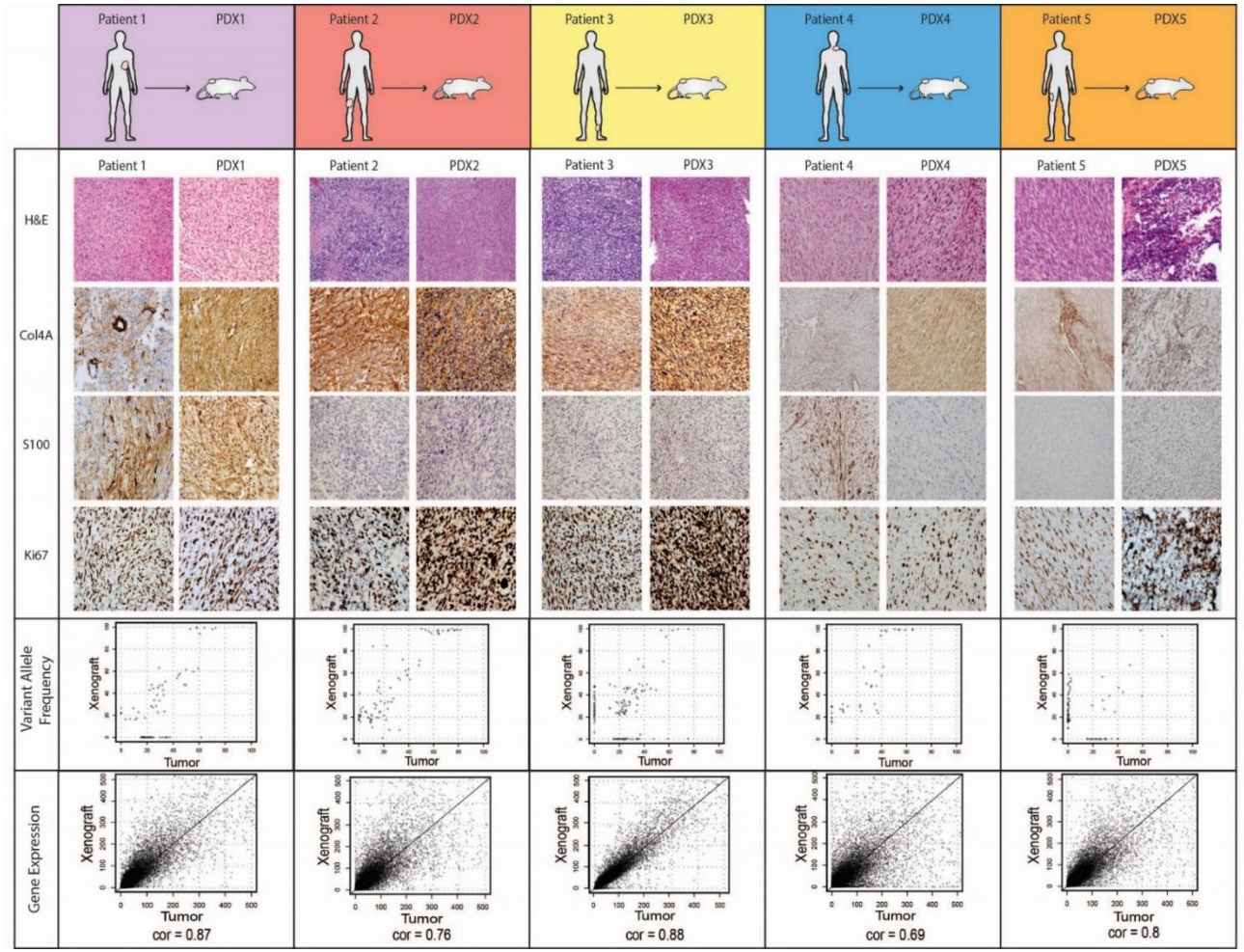

NTAP

NF Research Initiative

Boston Children's Hospital
Until every child is well

GeM Consortium
Genomics of MPNST

Potential Subsets?

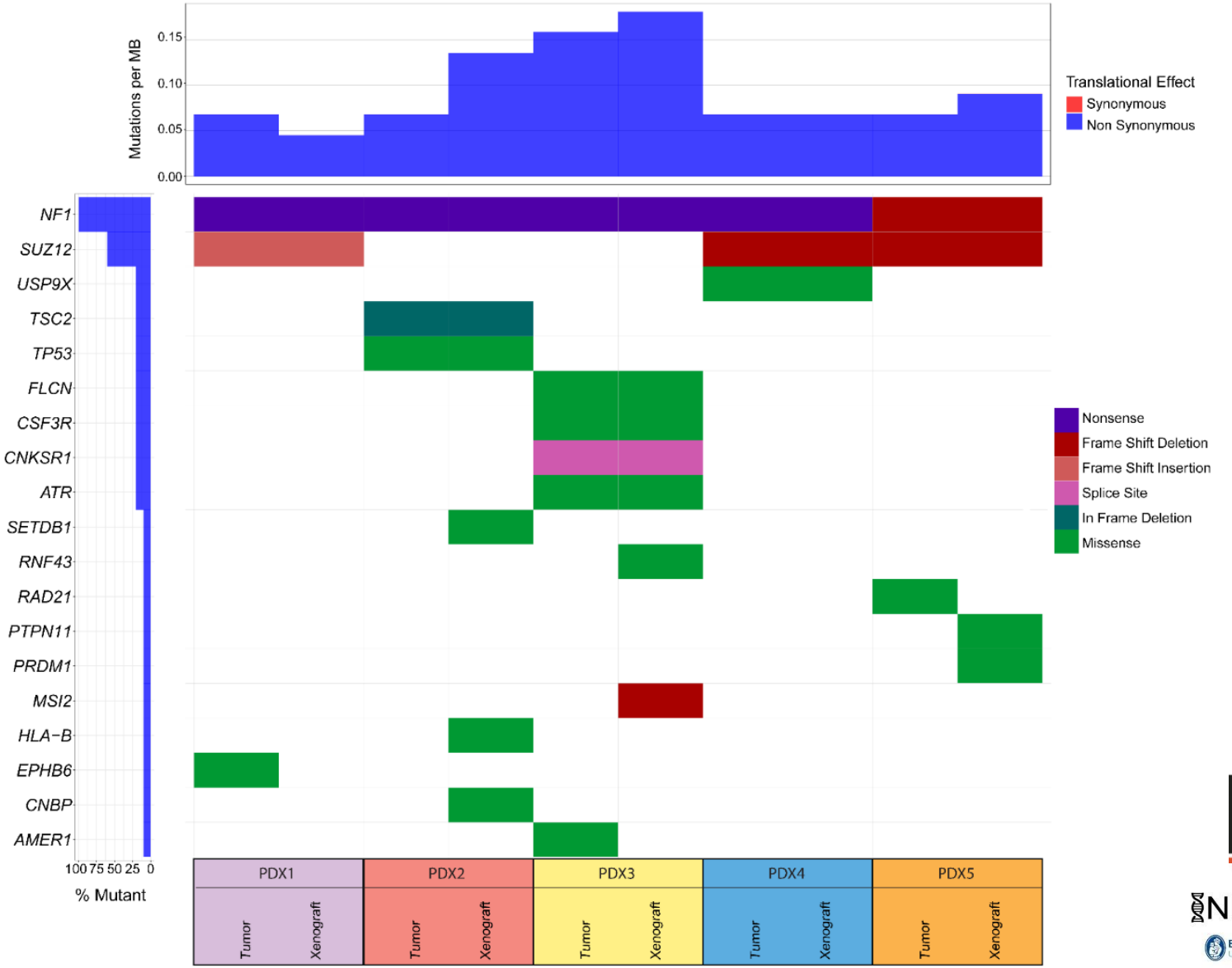

NTAP

NF Research Initiative

Boston Children's Hospital

GeM Consortium

Differential Response to Therapy

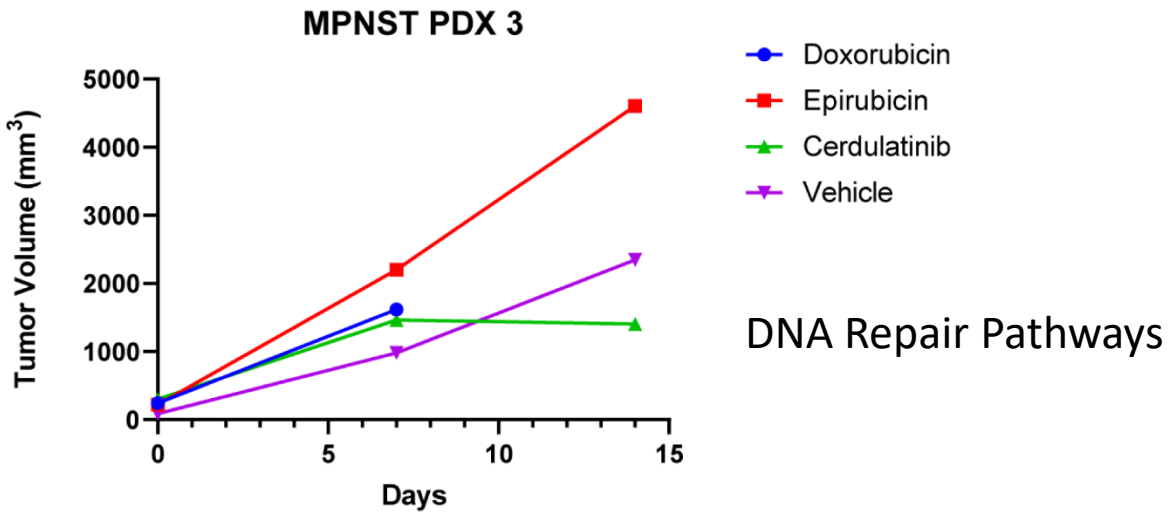

DNA Repair Pathways

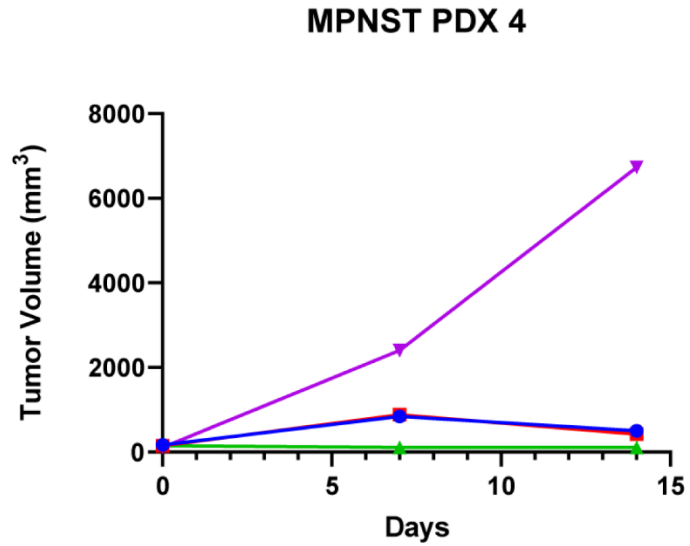

PRC2 Complex

NTAP

NF Research Initiative

Boston Children's Hospital
Until every child is well

GeM Consortium
Genomics of MPNST

Development of the MPNST Drug Testing Center and Data Coordination Center

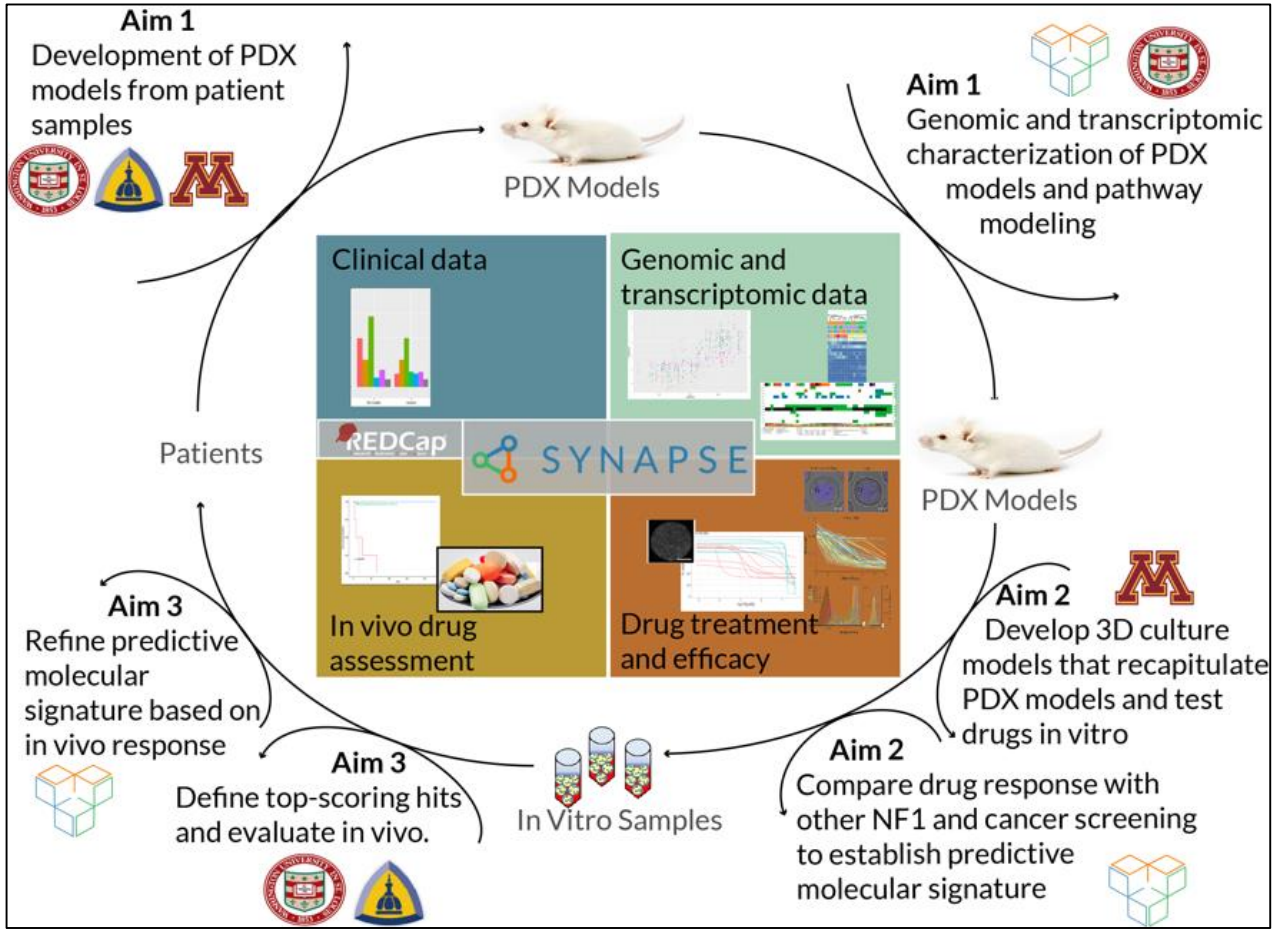

Table 1: Current MPNST PDX Lines from Washington University, Johns Hopkins University, and University of Minnesota

Tumor ID	Age (yrs)	Sex	NF1 status	MPNST	Histologic Grade	Anatomic Location	Size (cm)	Clinical Status
MPNST PDX 1	27	M	NF1	Primary	High	Mediastinum	12.6	Deceased
MPNST PDX 2	38	M	NF1	Primary	High	Thigh	22	Deceased
MPNST PDX 3	49	F	NF1	Primary	High	Calf	13.5	NED
MPNST PDX 4	34	M	NF1	Primary	High	Neck	7	NED
MPNST PDX 5	36	M	NF1	Primary	High	Thigh	15.8	NED
MPNST PDX 6	37	F	NF1	Primary	High	Pelvis	11	Deceased
MPNST PDX 7	52	M	NF1	Primary	High	Humerus	18	NED
MPNST PDX JH2-002	9	M	NF1	Primary	High	Pelvis	5.8	NED
MPNST PDX JH2-023	25	M	NF1	Primary	High	Paraspinal	6	NED
MPNST PDX JH2-031	12	M	NF1	Primary	High	Retroperitoneal	10	Deceased
MPNST PDX JH2-055	10	F	NF1	Primary	High	Scalp/ neck		NED
MPNST PDX MN1	22	F	NF1	Metastatic	High	Left Lung	NA	Deceased
MPNST PDX MN2	67	F	NF1	Primary	High	Maxillary Sinus	5.9	Pending
MPNST PDX MN3-001	21	M	NF1	Primary	Low	Left Gluteal	8	NED
MPNST PDX MN3-002	21	M	NF1	Primary	Low	Left Gluteal	8	NED

Scientific Plan Overview

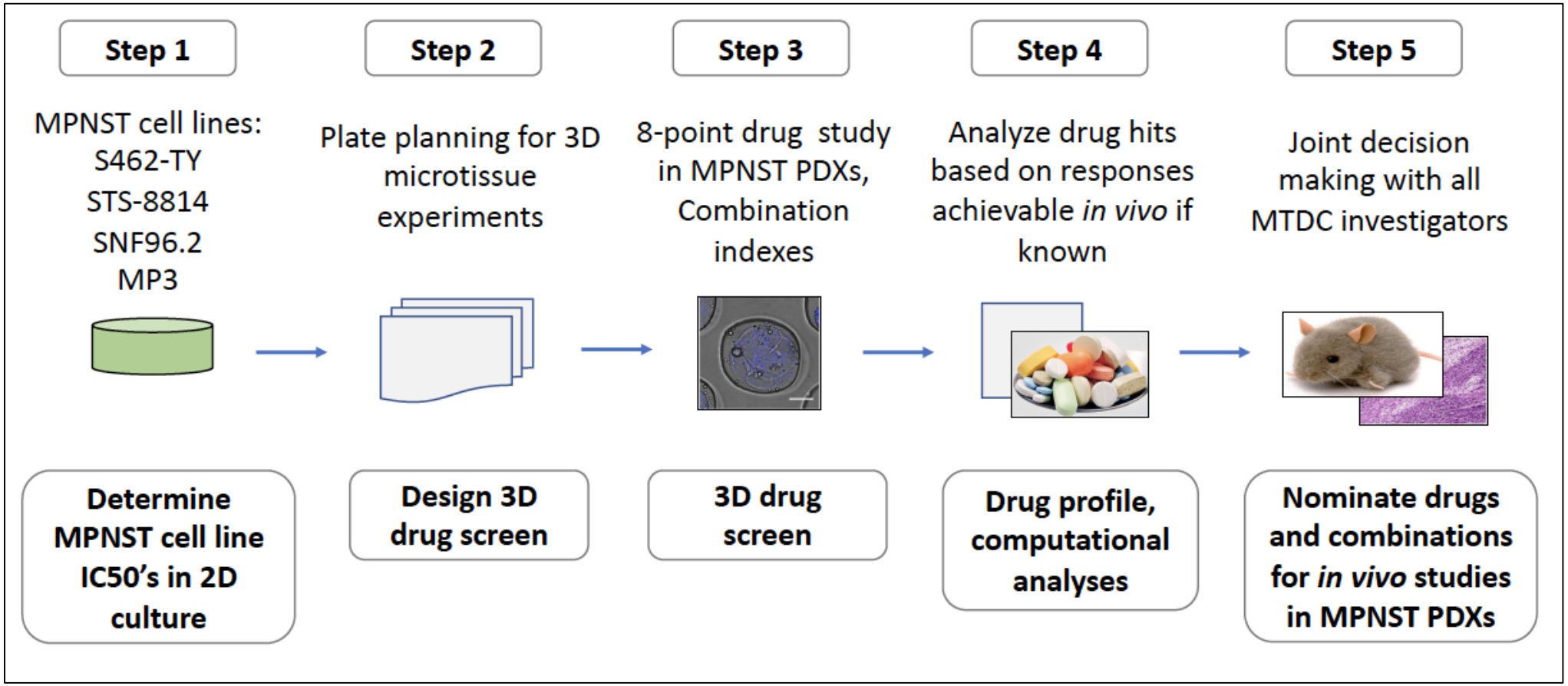

High Throughput Screening

- **Collagen microtissue fabrication.** (A) A chilled flow-focusing device partitions collagen-cell solution with an oil-surfactant phase, producing tens of thousands of 300 µm diameter collagen droplets per hour. (B) Droplets are placed at room temperature for 30 minutes to polymerize. Oil is then removed and tissues are resuspended in culture media prior to transfer to a microwell plate. (C) Once polymerized the microtissues can be cyropreserved or placed in microwells for growth assays. (D) Collagen microtissues of MPNST PDX cells after 7 days of culture reveals proliferation. Cells were plated at 3 cells per microtissue, but have clearly proliferated. (E) After 7 days of culture MPNST PDX cells are visualized using NucBlue staining. (F) Dead MPNST PDX cells are visualized using Sytox staining.

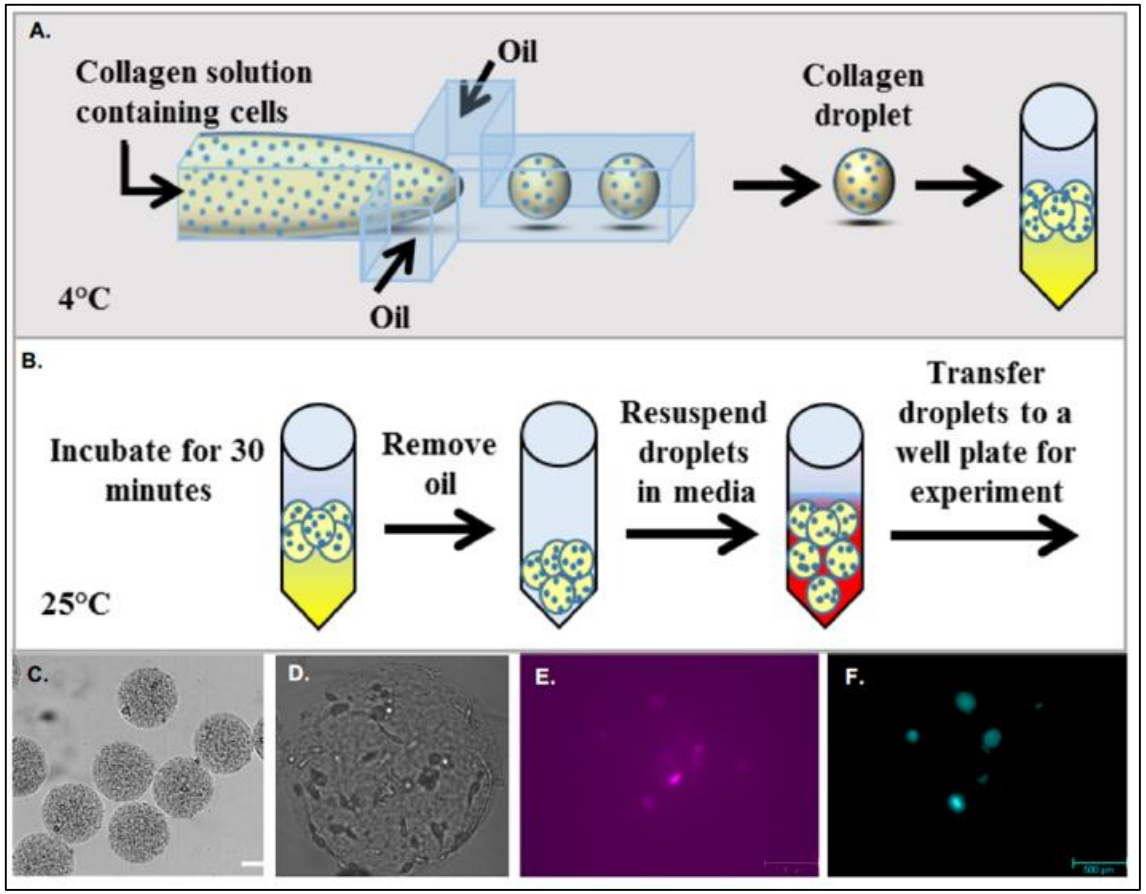

Possible Therapies to Test

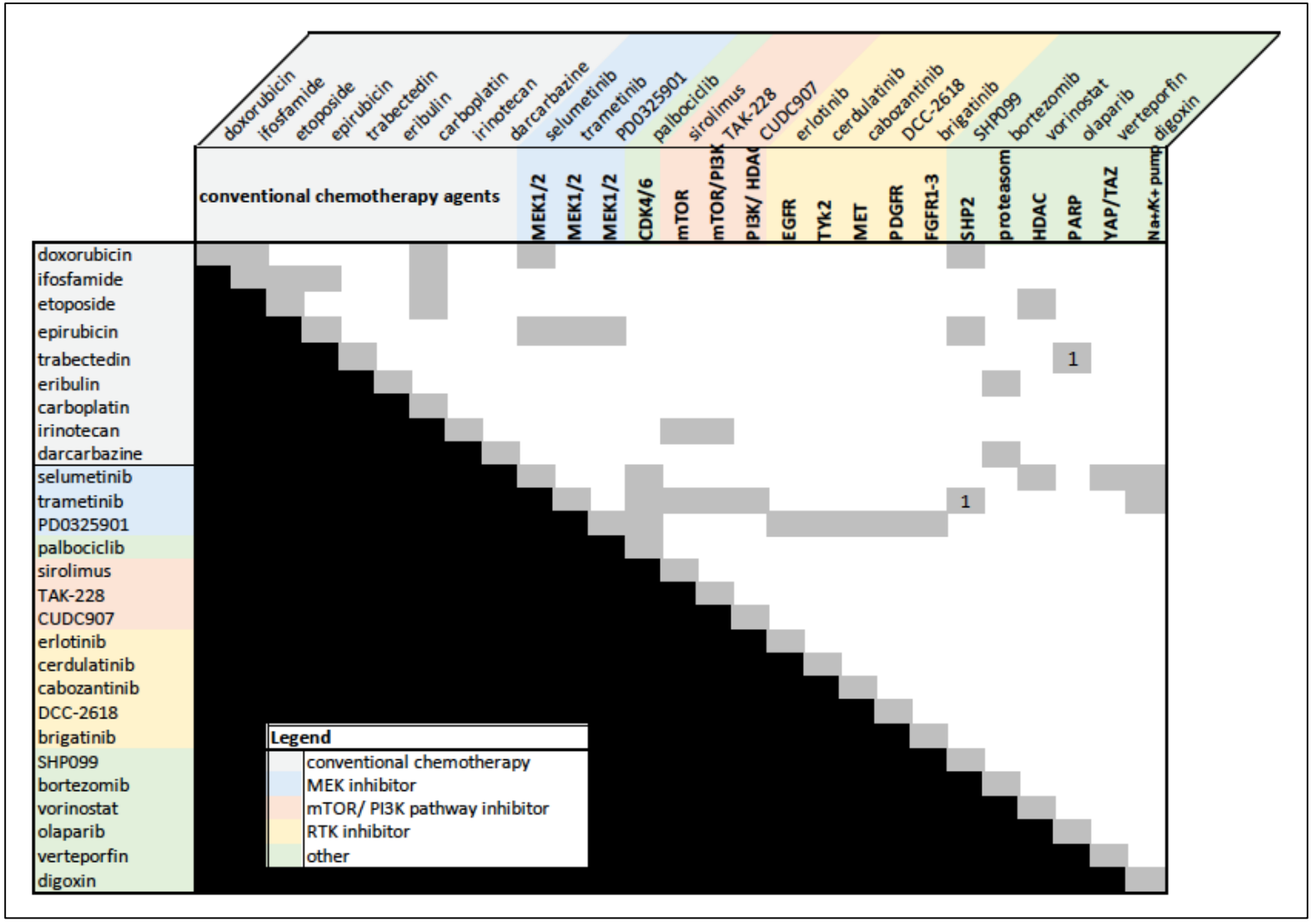

Promising Combinations to test *in vivo*

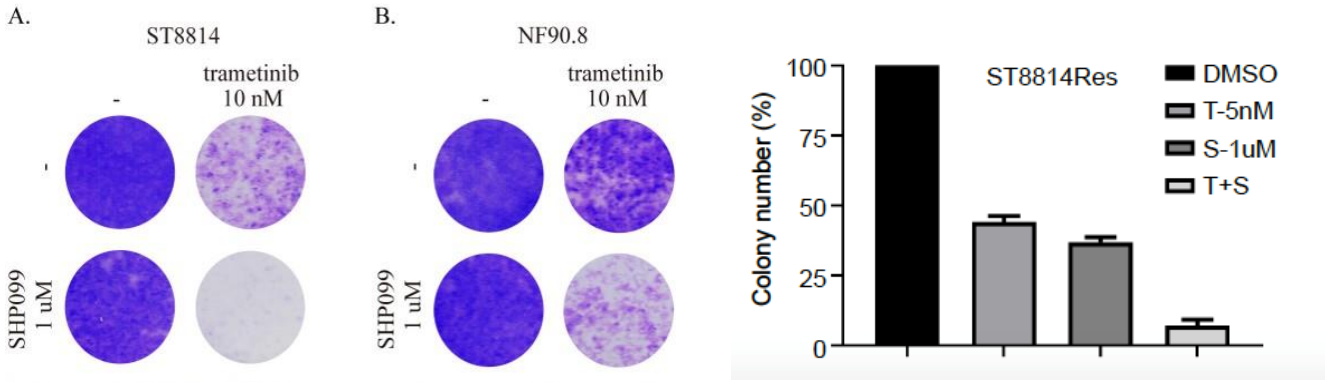

Pratilas Lab

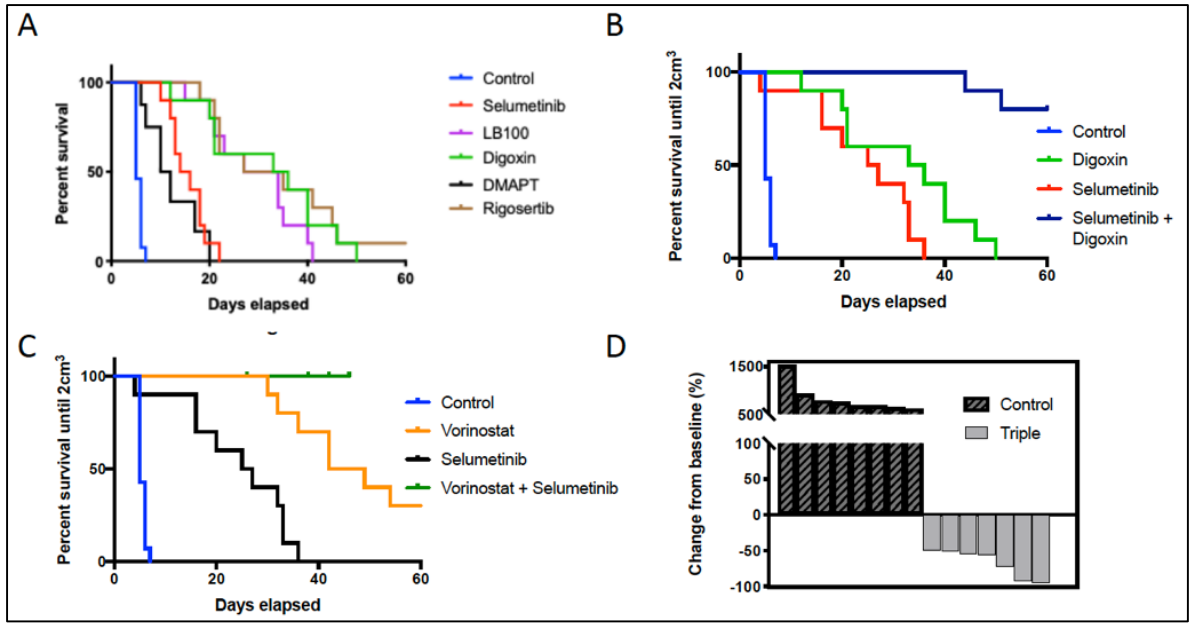

Largaespada Lab

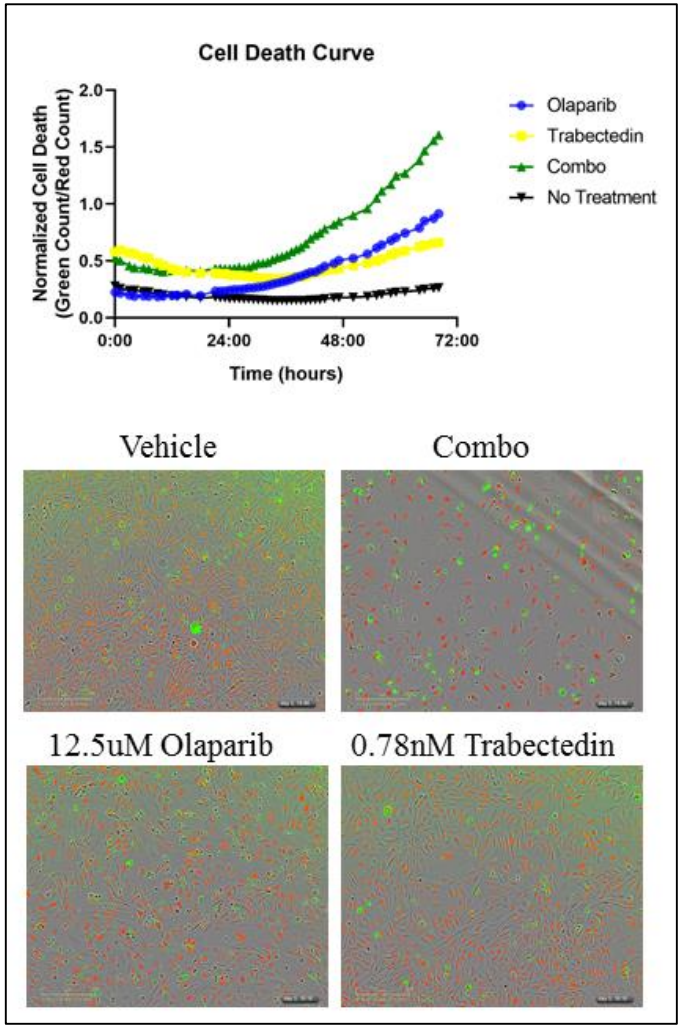

Hirbe Lab

Table 1 Frequency of somatic *NF1* mutations in different human neoplasms

Neoplasm	Frequency of somatic *NF1* mutations	References
Cutaneous melanoma	12–30%	[49–51, 58]
Desmoplastic melanoma	45–90%	[60, 61]
Lung adenocarcinoma	7–11.8%	[65–67, 166, 176, 177]
Lung squamous cell carcinoma	10.3–11%	[72, 177]
Acute myeloid leukaemia	3.5–23.6%	[82–85]
T cell acute lymphoblastic leukaemia	3%	[88]
Breast cancer	2.5–27.7%	[106, 177]
Ovarian carcinoma	12–34.4%	[113, 115, 170, 177–180]
Paraganglioma/ phaeochromocytoma	21–26%	[121, 124, 177]
Neuroblastoma	2.2–6%	[130]
Glioblastoma	14–23%	[132, 134, 177]
Colon adenocarcinoma	3.8–6.25%	[143, 177]
Bladder transitional cell carcinoma	6–14%	[149, 167, 177]

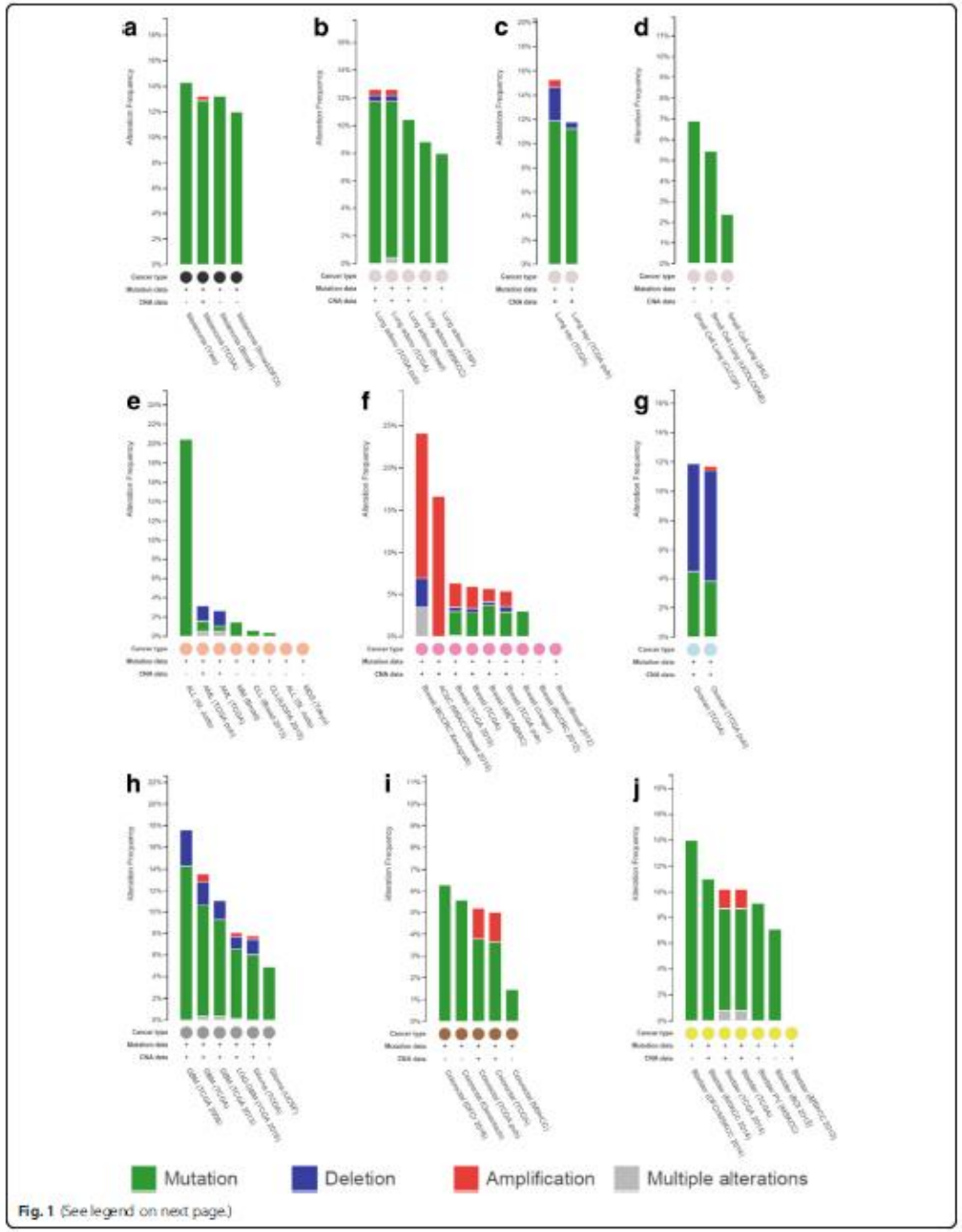

Fig. 1 (See legend on next page.)

Philpott et al. Human Genomics. 2017.

Summary

- *NF1* is a model tumor suppressor gene, mutated in the most common cancer predisposition syndrome.
- Patients with NF1 are at risk for numerous cancers, learning disabilities, bone abnormalities, and cardiac abnormalities.
- *NF1* is a critical gene involved in the development of sporadic cancers.
- *NF1* is critical for development of numerous organ systems.

We have come a long way, but we have so much more to learn!

- *NF1* is a huge gene!
- What are all of the ras independent functions?
- What other genetic modifiers contribute to the phenotype?
- Further understanding of the genomics and pathophysiology are essential to help us treat NF1 patients, sporadic cancers, and to understand normal development.

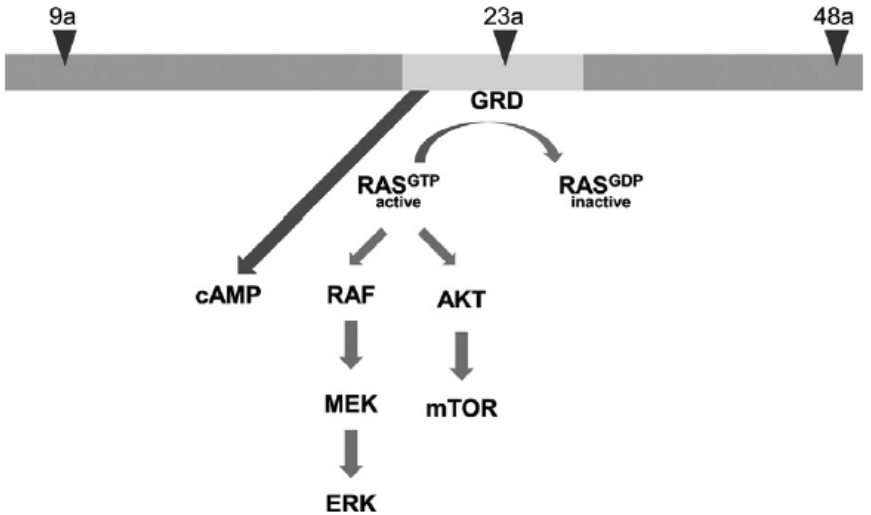

Cimino et al. Handbook of Clinical Neurology. 2018

Questions?

Cell, Vol. 63, 843–849, November 16, 1990,

The GAP-Related Domain of the Neurofibromatosis Type 1 Gene Product Interacts with *ras* p21

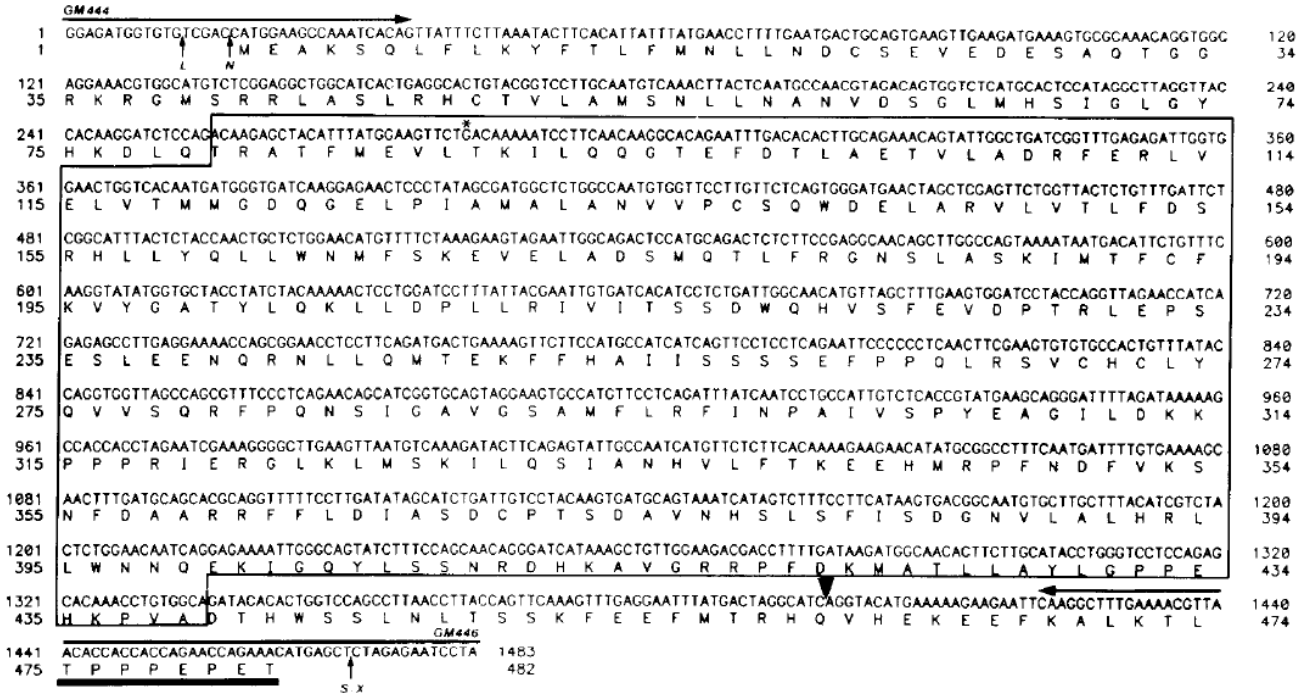

Figure 1. Nucleotide Sequence and Predicted Amino Acid Sequence of the GAP-Related Domain of NF1

The region of similarity between GAP and NF1 is boxed (Xu et al., 1990). Differences between this sequence and the previously reported sequence for NF1 (Xu et al., 1990) are indicated as follows: an asterisk indicates a guanosine residue that was previously reported as a cytosine residue; the amino acid sequence is unaffected by this difference; a black triangle indicates the position of three nucleotides from the previously reported sequence (ATC) that are not present in this sequence. Areas corresponding to PCR primers used to amplify the DNA from phage FB15 are overlined; arrows indicate the 5′ to 3′ direction of the oligonucleotides. Restriction enzyme cleavage sites used for subcloning are indicated by arrows (L = SalI, N = NcoI, S = SacI, X = XbaI). The bold underline indicates the epitope recognized by KT3 monoclonal antibody.

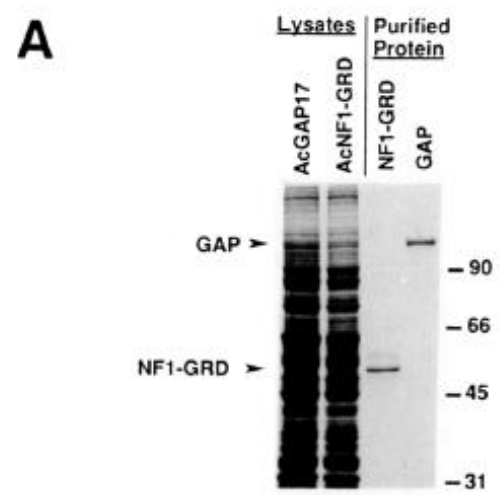
A
Lysates
Purified Protein
AcGAP17
AcNF1-GRD
NF1-GRD
GAP
GAP
NF1-GRD
90
66
45
31

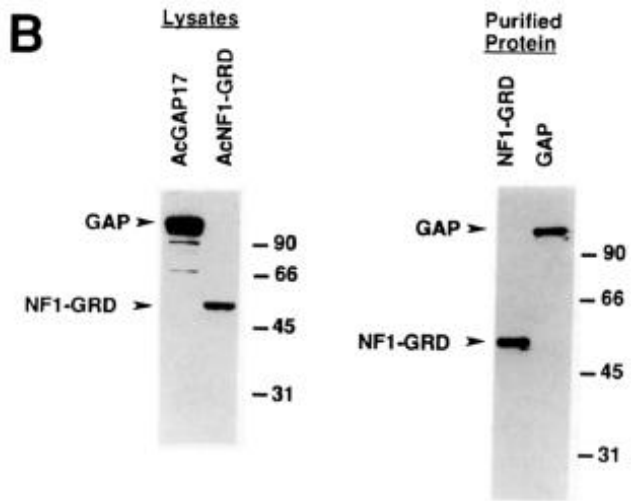
B
Lysates
AcGAP17
AcNF1-GRD
GAP
NF1-GRD
90
66
45
31
Purified Protein
NF1-GRD
GAP
GAP
NF1-GRD
90
66
45
31

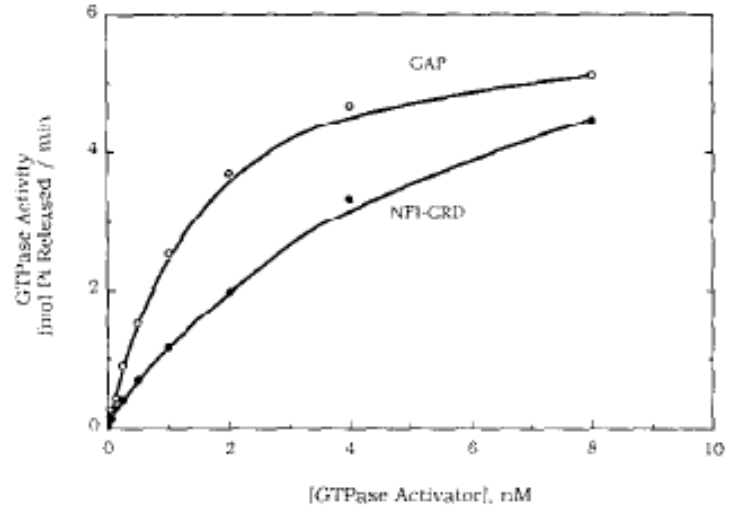
GAP
NF1-GRD
GTPase Activity
[mol Pi Released / min
[GTPase Activator], nM

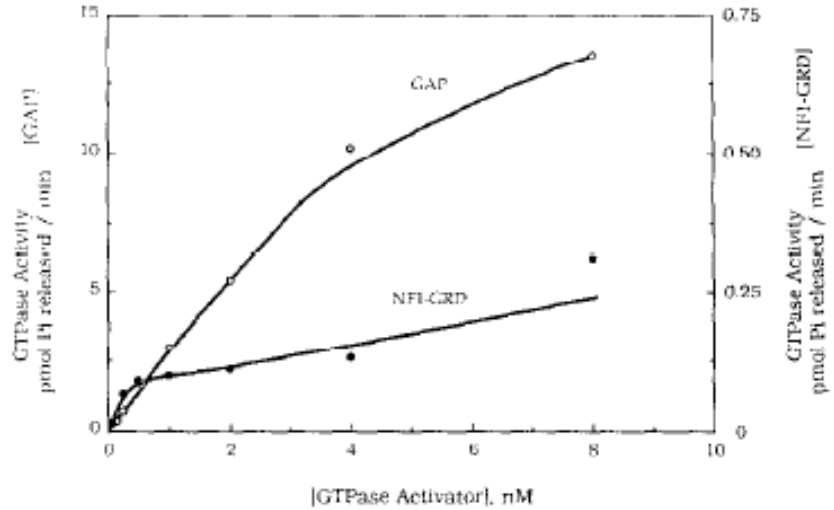
GAP
NF1-GRD
GTPase Activity
pmol Pi released / min
[GAP]
[NF1-GRD]
[GTPase Activator], nM

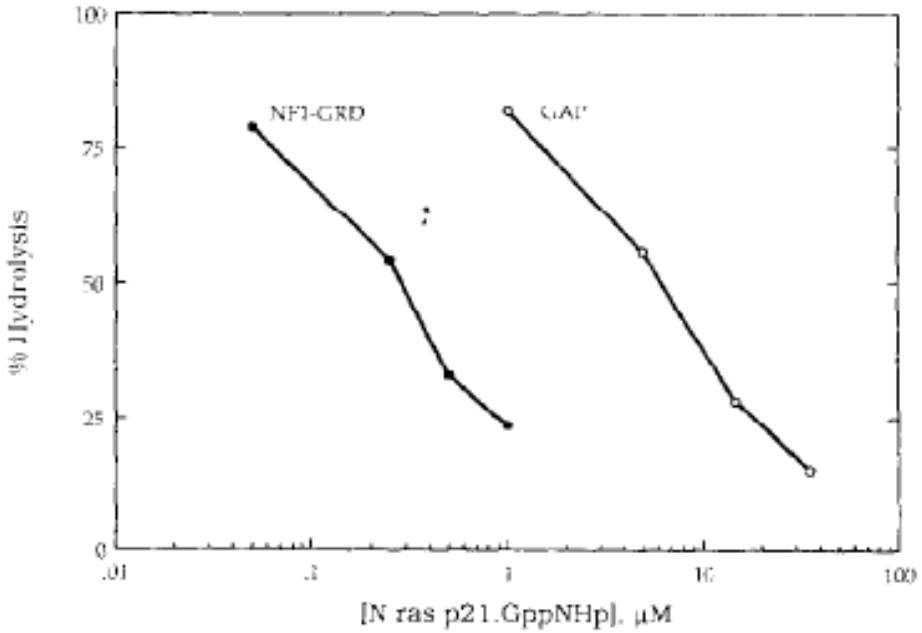

Figure 4. Competitive Inhibition by *ras* p21·GppNHp on Hydrolysis by NF1 GRD and GAP of *ras* p21·[γ-^{32}P]GTP

The concentration of *ras* p21·[γ-^{32}P]GTP was approximately 2 nM.

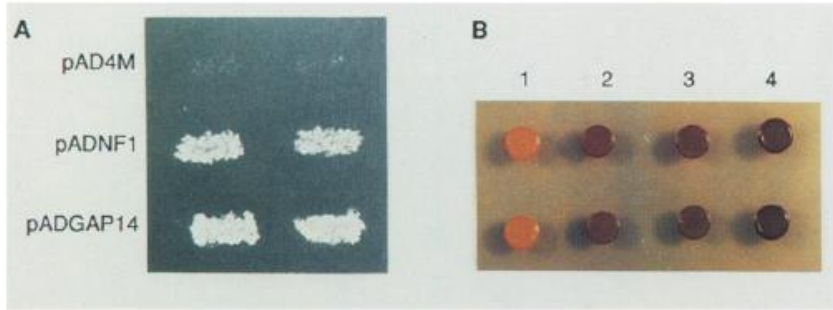

Figure 5. Effects of NF1 GRD on Heat Shock Sensitivity and Glycogen Storage in Yeast

(A) Yeast strain IR-1 (*ira1*$^-$) was transformed by plasmid pAD4M (vector control), pADNF1, or pADGAP14, and two independent transformants of each were grown on selective medium, replica plated, and subjected to heat shock as described in Experimental Procedures.

(B) Two independent transformants of (1) IR-1/pAD4M, (2) IR-1/pADNF1, (3) IR-1/pADGAP14, and (4) SP1/pAD4M were each spotted onto selective medium and grown for 36 hr at 30°C, then assayed for glycogen accumulation by staining with iodine vapors.

THE JOURNAL OF BIOLOGICAL CHEMISTRY

Vol. 268, No. 30, Issue of October 25, pp. 22331–22337, 1993
Printed in U.S.A.

The GTPase-activating NF1 Fragment of 91 Amino Acids Reverses v-Ha-Ras-induced Malignant Phenotype*

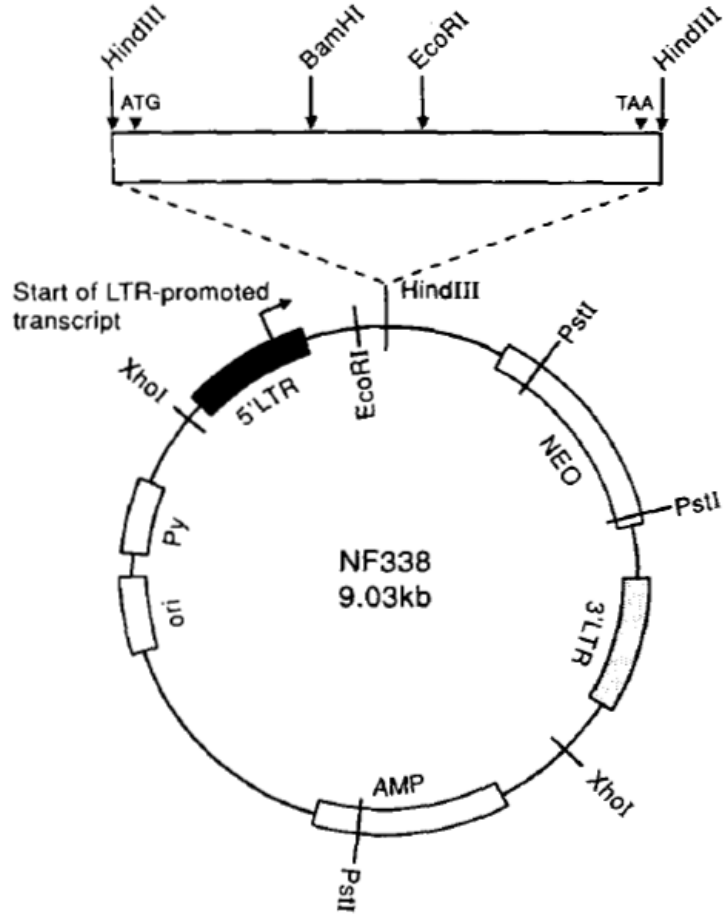

FIG. 1. **Construction of the plasmids NF338+ and NF338− expressing the NF1-GRD (sense (+) and antisense (−)).** A *Hin*dIII polymerase chain reaction fragment of 1.1 kilobases, encoding the NF1-GRD (residues 1194–1531) of human NF1, was subcloned into the vector pMV7, and the orientation of the insert was determined as described under "Materials and Methods." kb, kilobases.

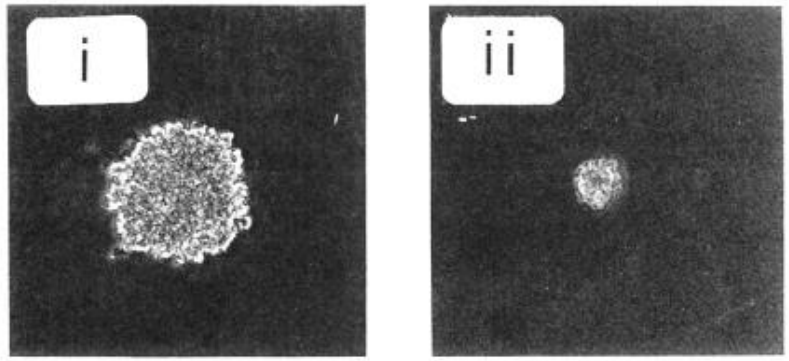

FIG. 2. **NF1-GRD-dependent inhibition of v-Ha-Ras-induced colony formation in soft agar.** *i*, nontransfected cells (clone 0); *ii*, NF1-GRD-expressing cells (clone 22). v-Ha-Ras-transformed NIH/3T3 cells were transfected with either NF338+ or NF338−, and the resultant G418-resistant transfectants were cloned as described under "Materials and Methods." Colony-forming ability of the parental clone and each transfectant was examined in a soft agar as described under "Materials and Methods."

TABLE I

Anti-oncogenic action of NF1-GRD and NF91 in v-Ha-ras-transformed NIH/3T3 cells

Clone	NF1-GRD or NF91[a]	Colonies/10^3cells[b]	SAC[c]
			%
0	None	735 (large)	100
8	GRD (sense)^L	37 (medium)	5
22	GRD (sense)^H	3 (small)	0.4
12	Anti-sense^H	910 (large)	124
17	NF91 (sense)^H	0	0
7	NF91 (sense)^L	10 (small)	1.3

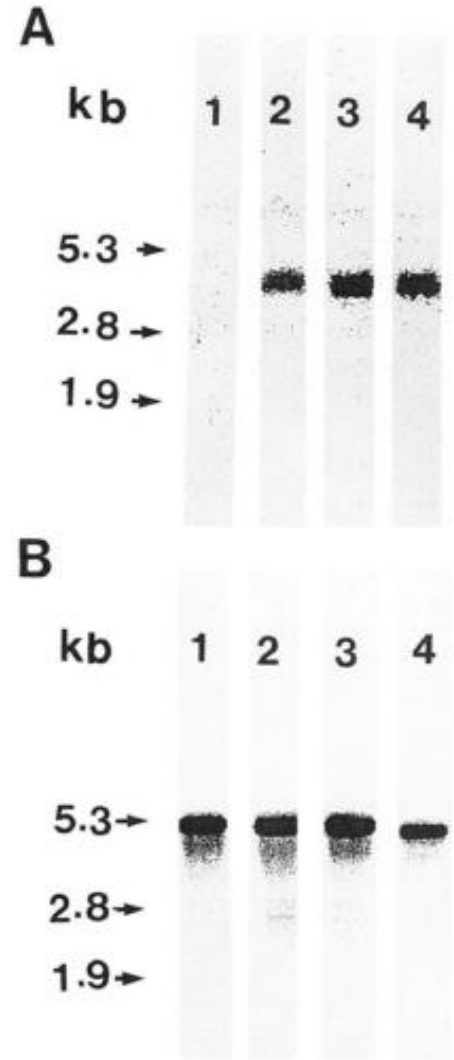

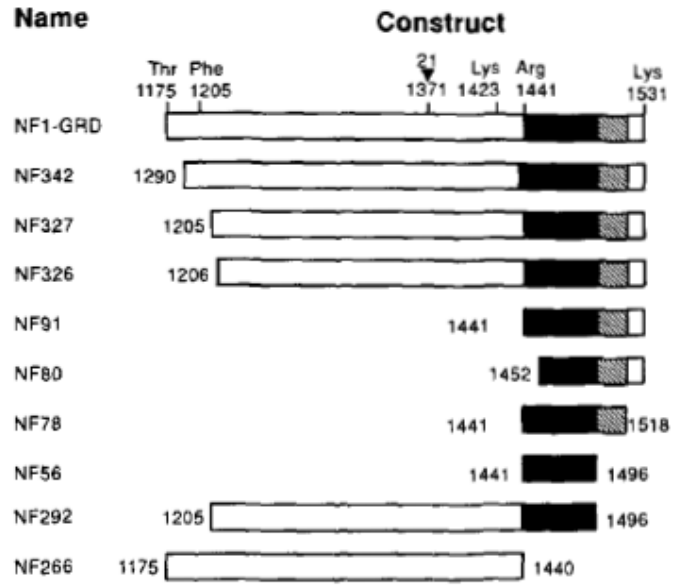

FIG. 4. **N- and C-terminal deletion mutants of the NF1-GRD (type I).** A series of the NF1-GRD mutants containing the indicated residues were produced as glutathione S-transferase fusion proteins and affinity-purified as described under "Materials and Methods." Their GAP (Ras GTPase-stimulating) activity is shown in Table II. The *number* following *NF* of each mutant indicates the total amino acid residues included. The type II-specific insert of 21 amino acids is indicated by the *number 21 above* the *arrowhead (top)* following the codon 1371. The *solid rectangles* indicate the GAP-active center of 56 amino acids, whereas the *shaded rectangles* indicate a supporting domain of 22 amino acids.

TABLE II

ras GTPase activation by NF1-GRD mutants

Hydrolysis of [γ-^{32}P]GTP (50 nM) bound Ha-ras protein was measured at 25 °C for 20 min in the absence or presence of each NF1-GRD mutant at various concentrations as described under "Materials and Methods."

NF1 constructs[a]	Activation[b]	EC_{50}[c]
	-fold	*μg/ml*
NF1-GRD, 1175–1531	14	0.50
NF 342, 1190–1531	14	0.52
NF 327, 1205–1531	14	0.40
NF 326, 1206–1531	11	1.5
NF 91, 1441–1531	10	10
NF 80, 1452–1531	0	
NF 78, 1441–1518	6	25
NF 56, 1441–1496	0	
NF 292, 1205–1496	11	7.5
NF 266, 1175–1440	0	

[a] For detail of the constructs, see Fig. 4.

[b] Activation of Ras GTPase by 20 μg/ml/ml NF1-GRD mutants.

[c] The NF1-GRD concentrations required for 50% hydrolysis of GTP bound to Ras. Each presented value was the average of the data from four to six independent experiments, and the standard deviations in each case was less than 5%.

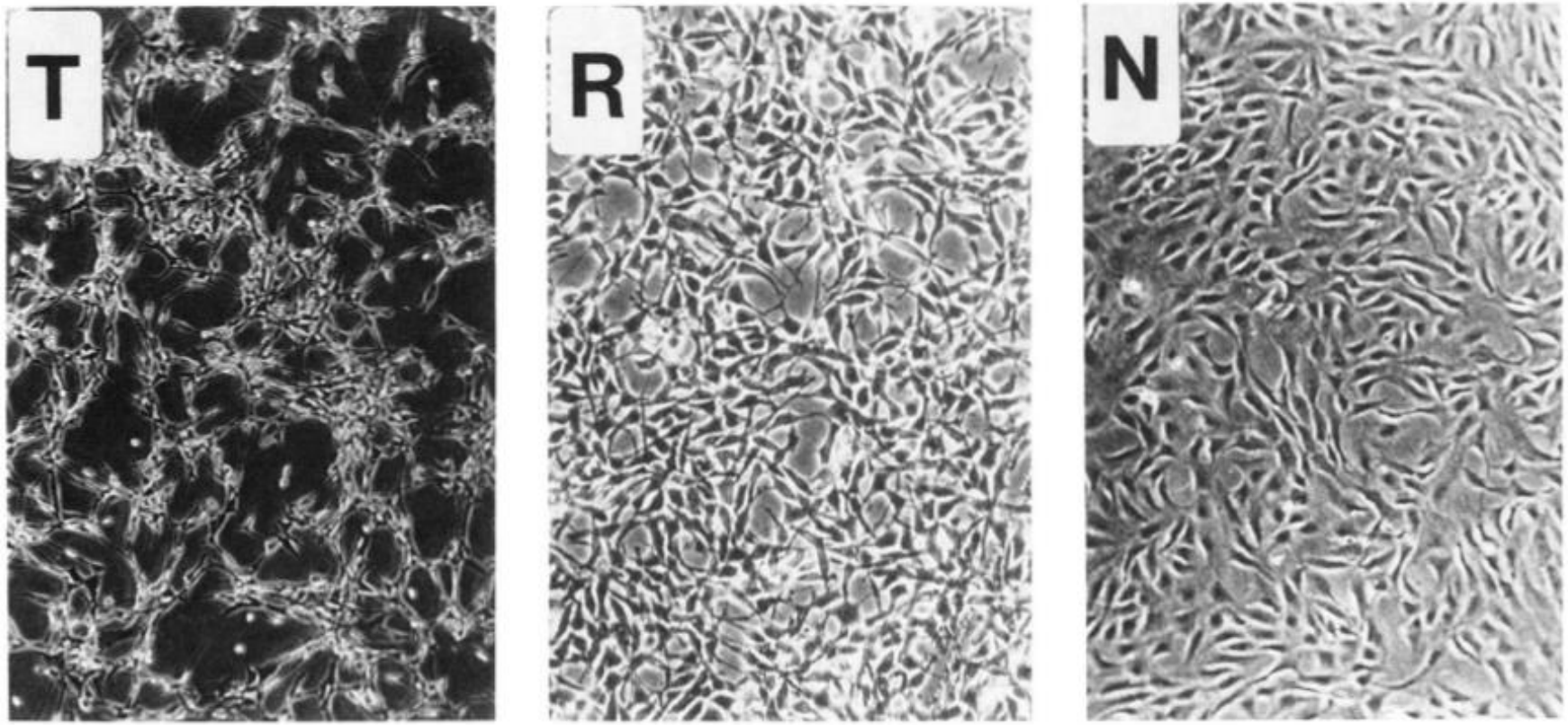

FIG. 5. **Morphological change of v-Ha-Ras-transformed cells by overexpression of the NF91.** *T*, v-Ha-Ras-transformed parental cells (clone 0); *R*, flat revertants (clone 17) derived from v-Ha-Ras-transformed cells transfected with the NF91; *N*, normal NIH/3T3 fibroblasts.